Thresholds for estuarine compound flooding using a combined hydrodynamic-statistical modelling approach

Charlotte Lyddon[1], Nguyen Chien[2], Grigorios Vasilopoulos[3], Michael Ridgill[4], Sogol Moradian[5], Agnieszka Olbert[5], Thomas Coulthard[3], Andrew Barkwith[6], Peter Robins[4]

[1]Department of Geography and Planning, University of Liverpool, UK
[2]School of Engineering, Edinburgh University, UK
[3]School of Environmental Sciences, University of Hull, Hull, England, UK
[4]School of Ocean Science, Bangor University, UK
[5]Civil Engineering, University of Galway, Ireland
[6]British Geological Survey, Keyworth, Nottingham, UK

Correspondence to: Charlotte Lyddon (c.e.lyddon@liverpool.ac.uk)

Abstract. Estuarine compound flooding can happen when an extreme sea level and river discharge occur concurrently, or in close succession, inundating low-lying coastal regions. Such events are hard to predict and amplify the hazard. Recent UK storms, including Storm Desmond (2015) and Ciara (2020), have highlighted the vulnerability of mountainous Atlantic-facing catchments to the impacts of compound flooding including risk to life and short- and long-term socioeconomic damages. To improve prediction and early-warning of compound flooding, combined sea and river thresholds need to be established. In this study, observational data and numerical modelling were used to reconstruct the historic flood record of an estuary particularly vulnerable to compound flooding (Conwy, North Wales). The record was used to develop a method for identifying combined sea level and river discharge thresholds for flooding using idealised simulations and joint-probability analyses. The results show how flooding extent responds to increasing total water level and river discharge, with notable amplification in flood extent due to the compounding drivers in some circumstances, and sensitivity (~7%) due to a 3-hour time-lag between the drivers. The influence of storm surge magnitude (as a component of total water level) on flooding extent was only important for scenarios with minor flooding. There was variability as to when and where compound flooding occurred; most likely under moderate sea and river conditions (e.g. 60-70th and 30-50th percentiles), and only in the mid-estuary zone. For such cases, joint probability analysis is important for establishing compound flood risk behaviour. Elsewhere in the estuary, either sea state (lower-estuary) or river flow (upper-estuary) dominated the hazard, and single value probability analysis is sufficient. These methods can be applied to estuaries worldwide to identify site-specific thresholds for flooding to support emergency response and long-term coastal management plans.

1 Introduction

Estuaries are the most dynamic coastal systems – crucial for global water and nutrient cycling, biodiversity of natural habitats, and provide ecosystem services such as food security and tourism that shape the livelihoods and well-being of their communities (Barbier et al., 2011). They hold strategic value for world trade, supporting haulage and fisheries, with significant growth opportunities, e.g., in marine energy. About 60% of the world's population lives along coastal and estuarine zones (Lindeboom et al., 2020) and 36% of the UK lives within 5 km of the coast (Census, 2020). Each year people make over 270 million recreational visits to UK coasts (Elliott et al., 2018) and generate £17.1 billion in tourist spend (NCTA, 2023). Sea-level rise and changing storm patterns, along with intensification of human activity in and around estuaries, e.g., littoralisation, farming, and water management, means estuarine communities are increasingly vulnerable to the impacts of extreme events – of which in the UK flood hazards are rated as the second highest risk for civil emergencies, after pandemic influenza, (HM Government, 2020; EA, 2023).

Estuaries are at the interface of marine (tide, storm surges, waves), hydrological and terrestrial (precipitation causing river discharge, runoff, snow melt, groundwater) physical processes, which interact over a range of temporal and spatial scales (Chilton et al., 2021). Standard terms follow the definitions outlined in Pugh (1987) and Chow et al. (1988). Flooding can occur when one or several of these processes cause water levels to exceed a critical threshold, such as a sea defence (EA, 2022). A threshold represents a meteorological, river and/or coastal condition at which flooding hazard increases (Sene, 2008). If a forecasted storm event could exceed the threshold then action to mitigate the hazard should be taken, for example, issue a flood warning. In the UK, coastal flooding has an annual cost of up to £2.2 billion for flood management and emergency response (Penning-Rowsell, 2015). Estuaries are particularly vulnerable to the effects of compound flood events when coastal and fluvial drivers can occur concurrently or in close succession to generate flooding (Svensson and Jones, 2004; Couasnon, et al., 2020; Bevacqua et al., 2020; Robins et al., 2021). High sea-levels can occur due to astronomical high spring tides and can be further exacerbated when they co-occur with storms generating large surges and waves at the coast. Alongside this, storms can generate heavy precipitation and lead to high fluvial and pluvial flows, which increases flood hazards within estuaries (Ward et al., 2018). A compound event caused devastating flood impacts in Lancaster, NW-England following Storm Desmond, 4–6 December 2015, due to extended heavy rainfall and river discharges coinciding with an incoming tide (Ferranti et al., 2015).

Statistical analyses of long-term data, e.g., from paired coastal and riverine gauge observations can show dependence between these drivers (Hendry et al., 2019; Camus et al., 2021; Lyddon et al., 2022) and can be used to examine the joint exceedance probability of estuary water levels based on when marine and terrestrial drivers are above the predefined thresholds (e.g., 95th or 99th percentile) (Kew et al., 2013, Salvadori et al., 2016). Estuaries on the west coast of Britain are more likely to experience co-dependent extreme events and compound flooding than those on the east coast, due to the prevailing southwesterly storm tracks that can bring extreme storm surges and concomitant rainfall – the generally short and mountainous west coast catchments causing river flows to increase quickly and coincide with the surge (Haigh et al., 2016). Beyond the floods in Lancaster, NW-England, Storm Desmond caused severe compound flooding across several estuaries of west and southwest Britain, amounting to over £500m in flood-related damages (Bilskie and Hagen, 2018; Matthews et al., 2018). Flooding in estuaries on the east coast of Britain is more likely to be driven by independent surge and rainfall events because the catchments tend to be larger with slower runoff times and easterly storms tend not to be coupled with heavy rainfall (Svensson and Jones 2002), although the generally longer durations of high river flows (e.g., several days for the Humber, NE-England) increases the chances of high discharge coinciding with high sea levels from a separate storm. Modelling studies have shown the likelihood and impacts of compound flooding at local (Robins et al., 2021) and national scales (Ganguli and Merz, 2019; Eilander et al., 2020; Feng et al., 2023; Eilander et al., 2023), but do not specify driver thresholds that lead to compound flooding and spatial variability in flooding of different driver combinations.

Defining critical driver thresholds for estuary flooding is crucial for the early detection and forecasting of flood events to issue timely warnings, for operational purposes such as emergency response, and for identifying vulnerable areas to focus intervention and coastal management strategies (EA, 2009). Early warning systems and appropriate planning measures are the most widely used and reliable tools to ensure community preparedness (Alfieri et al., 2012). Early warning systems and subsequent responses require a thorough understanding of hazard behaviour and classification, and knowing when a specific environmental condition will be passed to cause flooding is vital in this framework (Šakić Trogrlić et al., 2022). Terrestrial-driven floods and marine-driven floods are generally considered separately in operational flood risk assessments (e.g. CoSMoS, USA (USGS)), and there is currently a UK government policy gap in terms of estuary flood risk (EA, *pers. comm.*). Flood assessments show when a critical threshold is exceeded to cause either fluvial or coastal flooding, but do not consider compound events. Modelling statistical and probabilistic methods can contribute to an understanding of the unique response of each estuary to flood drivers, where catchment typology, tidal regime, and estuary characteristics influence the behaviour of the hazard. The same water level return period at a location within an estuary can be caused by different drivers and cause different flood extents, showing the importance of understanding a range of site-specific, compound event scenarios alongside their joint probability (Olbert et al., 2023).

This research aims to identify the coastal and fluvial conditions that lead to flooding in an estuarine system. The research will use a combination of historic records of flooding, instrumental data, statistical analyses, and numerical modelling tools to identify the combined driver thresholds which cause flooding, and which areas within the estuary are vulnerable to the compounding effects. The research is applied to the Conwy Estuary, North Wales (N-Wales) as an example of a mountainous, flashy catchment on the west coast of Britain which is vulnerable to the effects of storm-driven, compound flooding. The case study and methodology are described in section 2, which demonstrates how historic records of flooding are supplemented with online sources, instrumental data from a paired river and tide gauge, and results from an inundation model (section 3). Joint probabilities are assigned to coastal and fluvial conditions before results are considered in the context of wider flood hazard policy to improve the accuracy of flood records and flood hazard assessments in the context of future climate change and land use change for improved resilience of coastal communities (section 4).

2 Methods

2.1 Conwy Estuary, North Wales

The Conwy Estuary is a steep and mountainous catchment in N-Wales that has been shown to be one of the most vulnerable in Britain to compound events of extreme surges coinciding with extreme river flows (Lyddon et al., 2021). The estuary is macrotidal, which is common for the UK, with a 4-6 m tidal range. The semi-diurnal tide displays pronounced tidal asymmetry, characterised by short, fast flood tides and longer, slower ebb tides, which is typical of many macrotidal estuaries. Current speeds reach 1.3 m s^{-1} during the 2.75 hr flood, while ebb current speeds are 25-30% smaller (Jago et al., 2023). The estuary is subject to the effects of surge generating, low pressure Atlantic storms, elevating sea level up to 1.6 m above predicted levels. The towns of Llanrwst in the upper estuary, and Conwy and Llandudno in the lower estuary are vulnerable to this hazard, and communities, businesses, and transport networks are affected by several floods each year. Most notably, the primary road and rail network connecting north and south Wales runs through the Conwy Valley. Storm Ciara, 9 February 2020, exemplifies the complexities of compound flooding. Ciara atypically came from the north bringing intense rainfall (80 mm in 15 hrs) that inundated the estuary floodplains to capacity and held back by the rising spring tide plus 0.72 m surge. Record-breaking flows (529 m^3/s) in the main river ensued, causing widespread flooding (> 150 properties) and a 'backwater effect' that flooded transport links and caused power outages. There was no warning, so residents and landowners had no chance of activating safety measures. Flooding was recorded throughout the community in local and regional news outlets (BBC, 2020; Evans, 2020; Spridgeon, 2020).

The Conwy Estuary has a record of instrumental, observation data available from the Cwmlanerch river gauge (https://nrfa.ceh.ac.uk/data/station/info/66011) and Llandudno tide gauge (https://ntslf.org/tgi/portinfo?port=Llandudno). River discharge recorded at Cwmlanerch is available at a 15-minute temporal resolution from November 1980-February 2023, with 99% data coverage in time. The total water level recorded at Llandudno is available at a 15-minute temporal resolution from January 1994-December 2020, with 88% data coverage in time. Total water level from the Llandudno tide gauge was linearly detrended to remove the effects of a historical sea level trend from the time series (Coles 2001). Historic records of flooding extend back to the 1980's before the instrumental tide gauge data began, therefore tide and surge reanalysis data for this period were obtained from the Global Tide Surge Model (GTSM). The third-generation GTSM (Kernkamp et al., 2011) has a coastal resolution of 1.25 km within Europe and is forced with meteorological fields from the ERA5 climate reanalysis to simulate extreme sea levels for the period 1979 to 2017. The tide and surge model has shown good agreement between modelled and observed sea-levels, and is applicable to flood risk and climate change research (Muis et al., 2016; Muis et al., 2020; Wang et al., 2022). The record length used in the analysis here is determined by the monitoring and modelling duration.

2.2 Historic records of flooding in Conwy

Natural Resource Wales (NRW) has collated information on Recorded Flood Extents to show areas that have flooded in the past from rivers, the sea or surface water, which is documented on an open-source, online data catalogue (NRW, 2020). The database of polygons (Figure 1a) shows 22 Recorded Flood Extents in the tidally-influenced Conwy estuary. Of these Recorded Flood Extents, 14 events were driven by high sea levels or river flows or both that caused flooding by channel capacity exceedance or overtopping of defences (i.e., ignoring flooding due to obstructions, blockages, local drainage issues, and excess surface water was ignored). Instrumental river gauge data was only available for six of these 14 events. The behaviour of the drivers of the six Recorded Flood Events was reconstructed from the sea level and river flow data records, including timing and magnitude of peak river discharge ($Qmax$), total water level ($TWLmax$), predicted tide level, and skew surge that preceded the flood (e.g., Figures 1e and 1f). Figures 1c and 1e show the 21 November 1980 compound event where $Qmax$ was recorded as 428 m^3/s at 03:45 am. $TWLmax$ was 4.5 m at 22:00 am (which included a 0.25 m skew surge); however lack of exact information on the timing of the flooding makes it difficult to determine if $TWLmax$ contributed to flooding, and whether this was a compound flood. The NRW catalogue notes that there was widespread flooding in the Conwy Valley at this time, although since this was the pre-internet era there are no further online records. Figures 1d and 1f show the 26 December 2015 compound event where $Qmax$ was recorded as 753 m^3/s at 10:45 am, and $TWLmax$ was 4.3 m at 11:00 am (which included a 0.3 m storm surge). The short, 15-minute time lag between $Qmax$ and $TWLmax$, and extreme magnitudes ($Qmax$ was an 85^{th} percentile event and $TWLmax$ was an 84^{th} percentile event), caused extensive flooding in Llanwrst and across the valley (ITV, 2015; Welsh Government, 2015; Jones, 2016; NRW, 2016); however, the Recorded Flood Event in the NRW catalogue covers only a small area at Llanwrst (Figure 1d). This suggests that historic records of flooding in the Conwy are incomplete, hence there is a need for further information on the drivers and impacts of flooding from which to establish flood prediction patterns and thresholds. NRW identifies that the absence of a Recorded Flood Extent does not mean the area has not flooded. This information gap is expected throughout the UK.

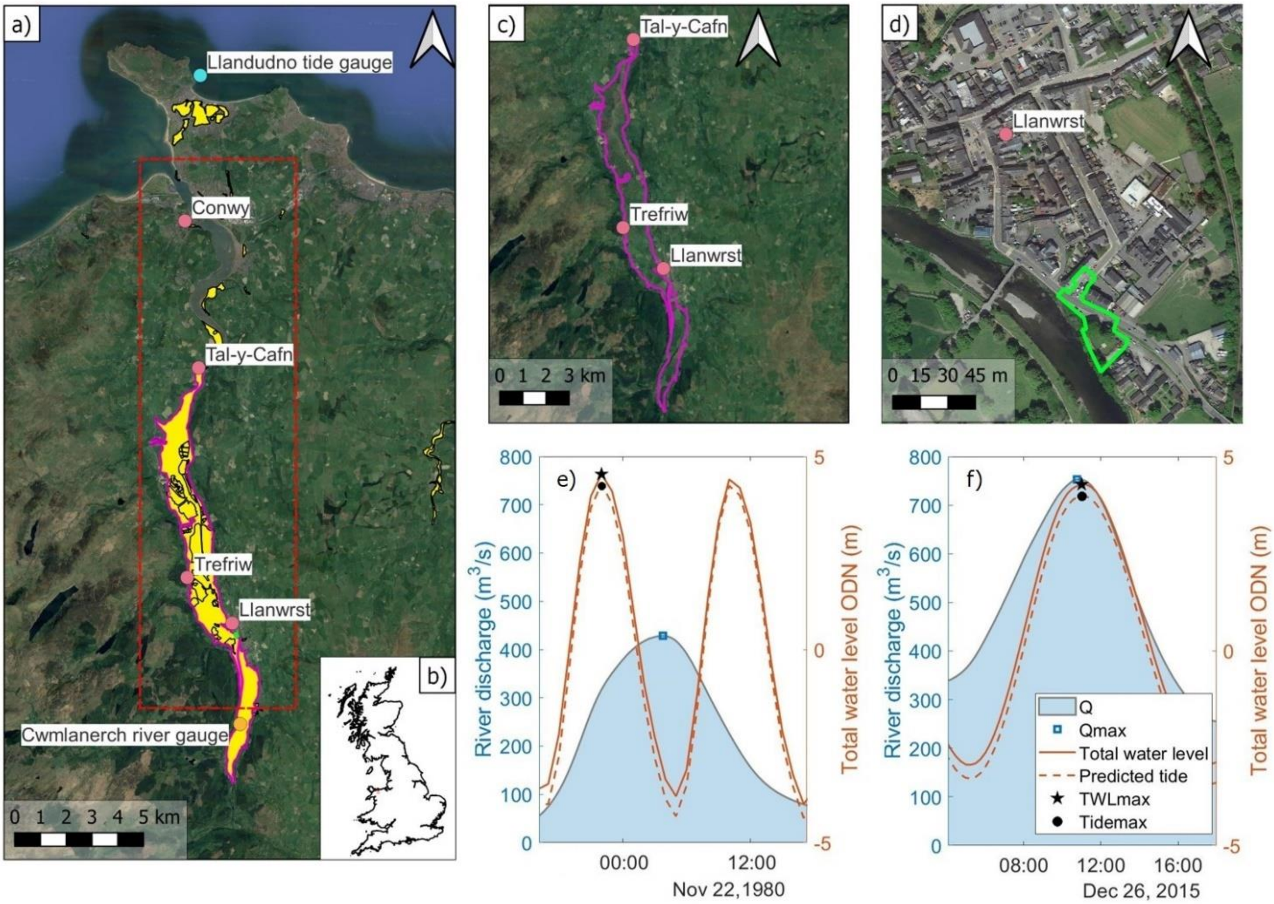

Figure 1: (a-b) Location and extent of all Recorded Flood Events (yellow shading) in the region of interest (red dashed box) in the Conwy Estuary, N-Wales. The outlines of two Recorded Flood Events are highlighted; 21 November 1980 (pink polygon) and 26 December 2015 (green polygon), which are shown in more detail in (c) and (d). (e-f) Time series of river discharge, total water level and predicted tide for two Recorded Flood Events in (c) and (d). Figure 1a-c Basemap © OpenStreetMap 2023

Flood drivers *Qmax* and *TWLmax* during the six Recorded Flood Events in NRW's data catalogue are shown as stars in Figure 2. Additionally, from analysis of the ~40 years of river/sea gauge data (see Section 2.1), the top 50 most extreme *Qmax* and corresponding *TWLmax* events within a 'storm-window' are shown as circles in Figure 2 (each of these corresponding events occur within a 'storm-window' of one another, defined as 20.25 hours for the Conwy based on the average duration of extreme event hydrographs over a 30-year period; Lyddon et al., 2021).Gaps in the tide gauge record meant that in effect the top 72 *Qmax* events were selected, to identify 50 events paired with *TWLmax*. Similarly, the top 50 most extreme *TWLmax* and corresponding *Qmax* events are shown as triangles in Figure 2. For all paired events plotted, the time lag in hours between *Qmax* and *TWLmax* is represented by the shape colour, and the vertical black line indicates the magnitude of the skew surge. One top 50 *Qmax* event corresponded with a top 50 *TWLmax* event, so that 99 extreme events were identified. Not all of these 99 extreme events from the gauge records necessarily caused flooding but this data highlights that there are potentially many events that caused flooding that are not recorded, as explored below. Further, two of the six Recorded Flood Extents corresponded with the 99 extreme events, meaning a total of 103 events are plotted in Figure 2.

The recorded most extreme *Qmax* was 901.31 m^3/s, which occurred on 16 March 2019, and coincided with a *TWLmax* of 6.57 m (a neap tide reaching 6.08 m combined with a 0.49 m skew surge), where there was a time lag of +3½ hrs (i.e., *Qmax* occurred on the ebbing tide). The relatively long time lag and less extreme *TWLmax* means that this was predominantly a fluvial-driven event, rather than a compound event. Flooding was recorded across the UK including in the Conwy on this date following a particularly wet period that included two major storms, Freyer and Gareth (Met Office, 2019). The recorded most extreme *TWLmax* was 8.95 m (a spring tide of 8.47 m with a skew surge of 0.48 m), which occurred on 10 February 1997, and coincided with a *Qmax* of 311.52 m^3/s, where there was a +1½ hour time lag (again *Qmax* occurred on the ebbing tide). Whilst coastal flooding was recorded in the Conwy Tidal Flood Risk Assessment (HRW, 2008), there was no flooding recorded within the estuary so it is not considered as a compound event.

Of the top 50 *Qmax* events, 39 had a time lag of $\pm$2 hours or less, of which 14 events had a time lag of $\pm$1 hour or less, showing that concurrence of *Qmax* and *TWLmax* has occurred regularly in the past. Although there was only one occasion when a top 50 *Qmax* and top 50 *TWLmax* co-occurred, and this event had a time lag of about an hour. Seven of the top 50 *TWLmax* events had a time lag of $\pm$2 hours or less, of which two events had a time lag of +1 hour or less. It is also worth noting that all top 50 *TWLmax* events occurred around midday (10:30-12:15) or midnight (22:45-00:00). Spring high tides are phase-locked around midday and midnight for the Conwy region, hence increasing the chances of an extreme water level at these times.

Three standout events are circled in Figure 2 which could be interpreted as compound events, all with extreme river discharges (*Qmax* > 700 m^3/s and > 77th percentile), high total water levels (*TWLmax* > 4 m and > 84th percentile), and time lags under $\pm$1 hour. One of these three events is starred as a Recorded Flood Event on the NRW data catalogue (26 December 2015); however, the others are not. It is important to know whether all of these extreme events in fact caused flooding as one might expect, and which other extreme events in the ~40 year record led to flooding, to be able to establish meaningful thresholds for flood warning.

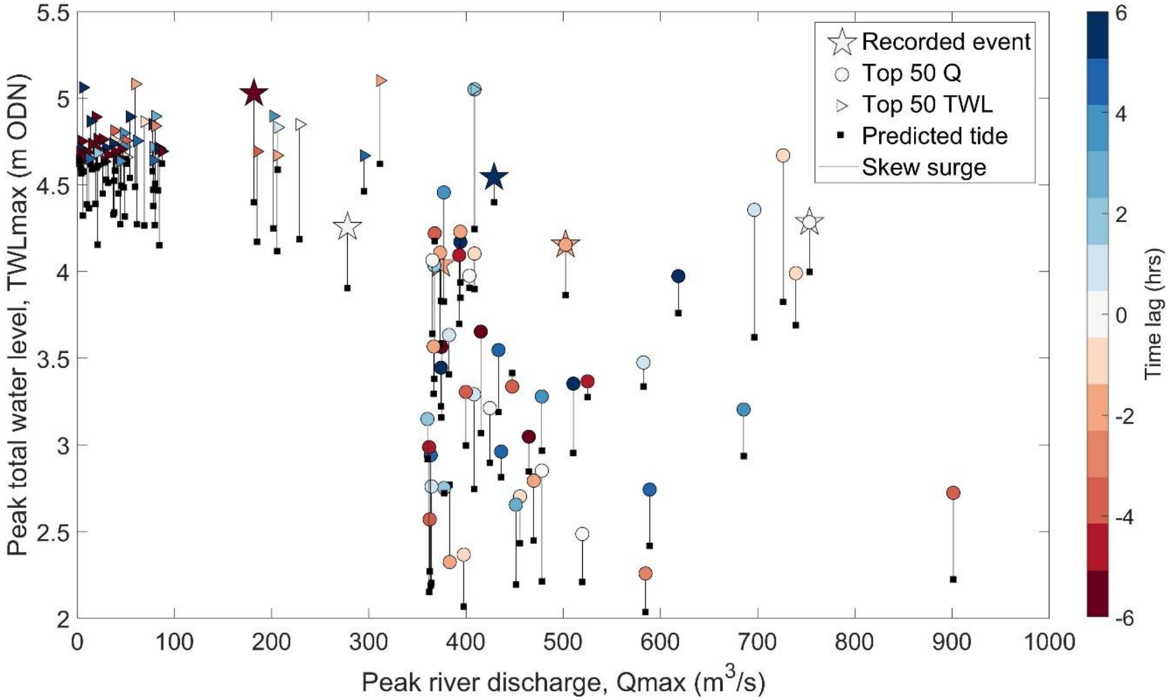

Figure 2: Recorded Flood Extents at Conwy (stars), top 50 *Qmax* events at Cwmlanerch (circles), top 50 *TWLmax* events at Llandudno (triangles), and associated predicted tide (black square) and skew surge magnitude (vertical black line) for each event. Colours indicate the length of time lag between peaks in river discharge and total water level (negative time lags indicate that *Qmax* arrived before *TWLmax* and so coincided with a flooding tide).

2.3 Extending the record of flooding

Records of historic flood events were expanded by exploring internet records. Online resources were used to identify if flooding happened as a result of extreme coastal and/or river conditions to create a more comprehensive record of historic flood events. Web scraping approaches (also referred to as web extraction or web harvesting) were used to evaluate whether there is further evidence of recorded flooding in the Conwy estuary within the 99 extreme *Qmax* and *TWLmax* events plotted in Figure 2. The dates of all recorded extreme events were searched on DuckDuckGo, Microsoft Bing, and Google. No evidence of flooding was available for events prior to 1990; online records prior to this date are unreliable and before the 'internet era'. Predetermined searches specified any evidence must be for an event in the Conwy Estuary from Deganwy upstream to Llanrwst (i.e. the dashed box in Figure 1a). Train and bus cancellations were also considered evidence of flooding events. A railway line runs between Deganwy and Llanrwst, stopping at Llandudno Junction, Glan Conwy, Tal-y-Cafn and Dolgarrog, so these stations were included in the web search. Results were supplied in browser tabs for analysis. If a date was deemed a 'flooding event', the supporting evidence was investigated to see if there was any information to note the drivers of the flooding (Table 1).

Table 1: Description of labels used to assign a cause of flood tag to a date

Label	**Code**
0	None
1	River discharge
2	Storm surge
3	High tide
4	Storminess

The web searches isolated an additional 26 recorded floods that matched extreme events in our analysis, as shown in Figure 3, with yellow circles indicating these 26 events. The blue circles in Figure 3 indicate extreme events where there was no online evidence of flooding. Labels assigned to three of the inundation events are shown in the figure. Multiple sources of evidence indicate a marine-driven flooding event on 3 January 2014, largely due to an extreme storm surge of 0.8 m, including railway cancellations, home evacuations, and road closures (Welsh Government, 2014; Sibley et al., 2015). Evidence of river-driven flooding on 16 March 2019, during Storm Gareth, was derived from news reports of damage to over 40 homes, road closures, and flood warnings issued by NRW (BBC, 2019; FloodList, 2019; Met Office, 2019). Evidence of river-driven and marine-driven flooding suggests that 9 February 2020 was a compound flood event. Figure 3 provides a more comprehensive record of flood inundation than shown in Figure 2; however, data gaps in instrumental time series, online evidence, and what information was recorded, leave uncertainty in where to set driver thresholds and patterns for flooding, especially for less extreme *Qmax* and *TWLmax* that led to compound flooding.

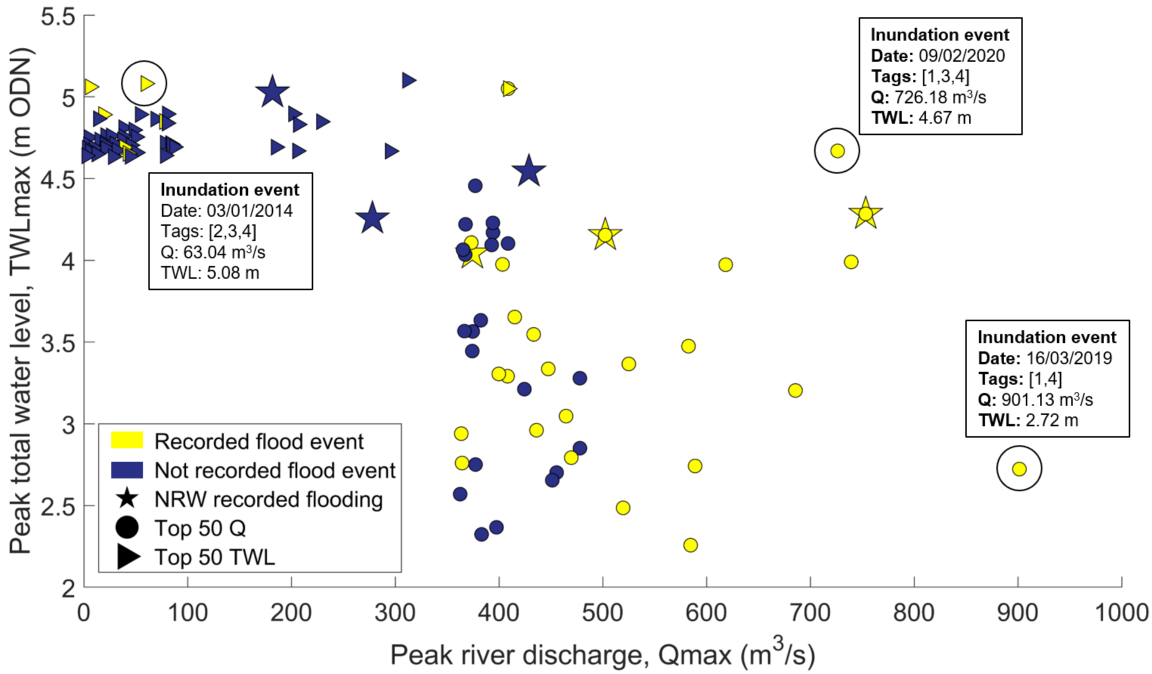

Figure 3: Recorded Flood Extents, and top 50 *Qmax* and top 50 *TWLmax* events, colour coded to show those events which were inundation events (yellow) and those which were non-inundation events (blue). Three events are highlighted to show drivers, timing, and labels for the cause of flooding.

2.4 Hydrodynamic inundation model

The Caesar-Lisflood hydrodynamic model (Coulthard et al., 2013; Skinner et al., 2015; Harrison et al., 2022) was used within a sensitivity test framework to simulate a series of idealised event scenarios which represent plausible combined river and sea level conditions, to identify which combination of drivers leads to flooding in the Conwy. CAESAR-Lisflood is a geomorphological and landscape evolution model that combines the Lisflood-FP 2D hydrodynamic flow model (Bates et al, 2010) with the CAESAR geomorphic model. Lisflood uses a flow routing algorithm that determines the direction of flow based on the elevation gradient, and conserves mass and partial momentum. CAESAR-Lisflood does not run in 3D, and this functionality is not required to explore flood inundation. Baroclinicity is not an important process to represent for this research, and would require additional computational expense.

2.4.1 Model domain

The model domain includes the tidally influenced Conwy estuary, downstream of the Cwmlanerch river gauge on the River Conwy and extending offshore into Conwy Bay and the Menai Strait at the coastal boundary. A number of sources were combined to generate the land elevation data required to build the model, including (a) seabed bathymetry, (b) land elevations and (c) location and heights of existing flood defences. The domain topography was based on the marine DEM, Lidar DTM and OS Terrain 5m DTM, all available through Digimap (https://digimap.edina.ac.uk/). The Lidar DTM data was used to check and, where necessary, augment the flood defences vector database,n obtained from the NRW data catalogue (https://datamap.gov.wales/). The processing steps undertaken to produce the model domain are described in Supplementary Information S1.

2.4.2 DEM calibration

Caesar-Lisflood was run in reach mode, in which the model is forced with discharge and water level time series at the upstream (river) and downstream (offshore) boundaries, respectively. For the upstream boundary, a time series of water discharge (m^3/s) measured at the Cwmlanerch gauge was used. The dataset provided by NRW has a 15-minute temporal resolution and covers the calibration period: 1 March-16 April 2021. For the offshore boundary, a time series of measured sea levels at Llandudno was used, provided by the British Oceanographic Data Centre (BODC). It contains measured levels above the Llandudno Chart Datum (CD) at 15-minute intervals and spans the same period as the time series of discharge. The tidal water levels were converted to Ordnance Datum (OD) by adjusting for the vertical offset between CD and OD (i.e. –3.85 m). The Manning's roughness coefficient for the river channels and marine areas was set to 0.022, the Courant number at 0.6 and the Froude limit at 0.8. To avoid water accumulation behind flood defences when overtopping occurred, a water loss function of 0.2 m day^{-1} was applied. The function was only applied to the floodplains to avoid affecting river or sea water levels. Only the hydrodynamic component of the model was used for the simulations described here and simulated water levels were exported at 15-minute intervals for further analysis.

Simulated water levels were compared against corresponding values obtained from gauges within the estuary at Pont Fawr, Trefriw and Tal-y-Cafn (see Figure 4). The gauges at Pont Fawr and Trefriw are maintained by NRW and monitor water levels at 15-minute intervals, relative to OD. At Tal-y-Cafn a pressure logger was installed in October 2020 (Lat. 53.23°N, Lon. 3.82°W) that also provided measured water levels, relative to OD at 15-minute intervals. Initially the DEM had incorrect channel bed elevations due to the LiDAR shortcomings for inundated areas (further detail in S1). We approximated the correct channel bathymetry by manually adjusting the channel bed elevations, re-running the simulation and comparing simulated and observed water levels. We repeated this process until we reached a satisfactory agreement between observed water levels and model predictions at the three gauges. With this method the bed profile is adjusted until it simulates the observed water profile taking into account flow non-uniformity (Neal et al., 2022). The calibrated DEM is shown in Figure 4a together with the locations of the various gauges used in the study. After the final DEM adjustment (Figure 4b), RMSE values were 0.59 m, 0.39 m, and 0.69 m (Figure 4c-e) for Pont Fawr, Trefriw and Tal-y-Cafn, respectively. Flood peaks were isolated in the calibration period and RMSE values were 0.57 m, 0.19 m, and 0.29 m for Pont Fawr, Trefriw and Tal-y-Cafn. Improved RMSE scores for flood peaks indicates the model is able to capture the magnitude of the largest and most prominent peaks. Higher RMSE values in the upper estuary (Pont Fawr gauge) could be attributed to the omission of tributaries in the model that flow into the Conwy downstream of the Cwmlanerch gauge (upstream boundary of the model). These inputs are, as a result, not represented in the discharge data forcing the model. Nevertheless the set up remains suitable for the purposes of this research

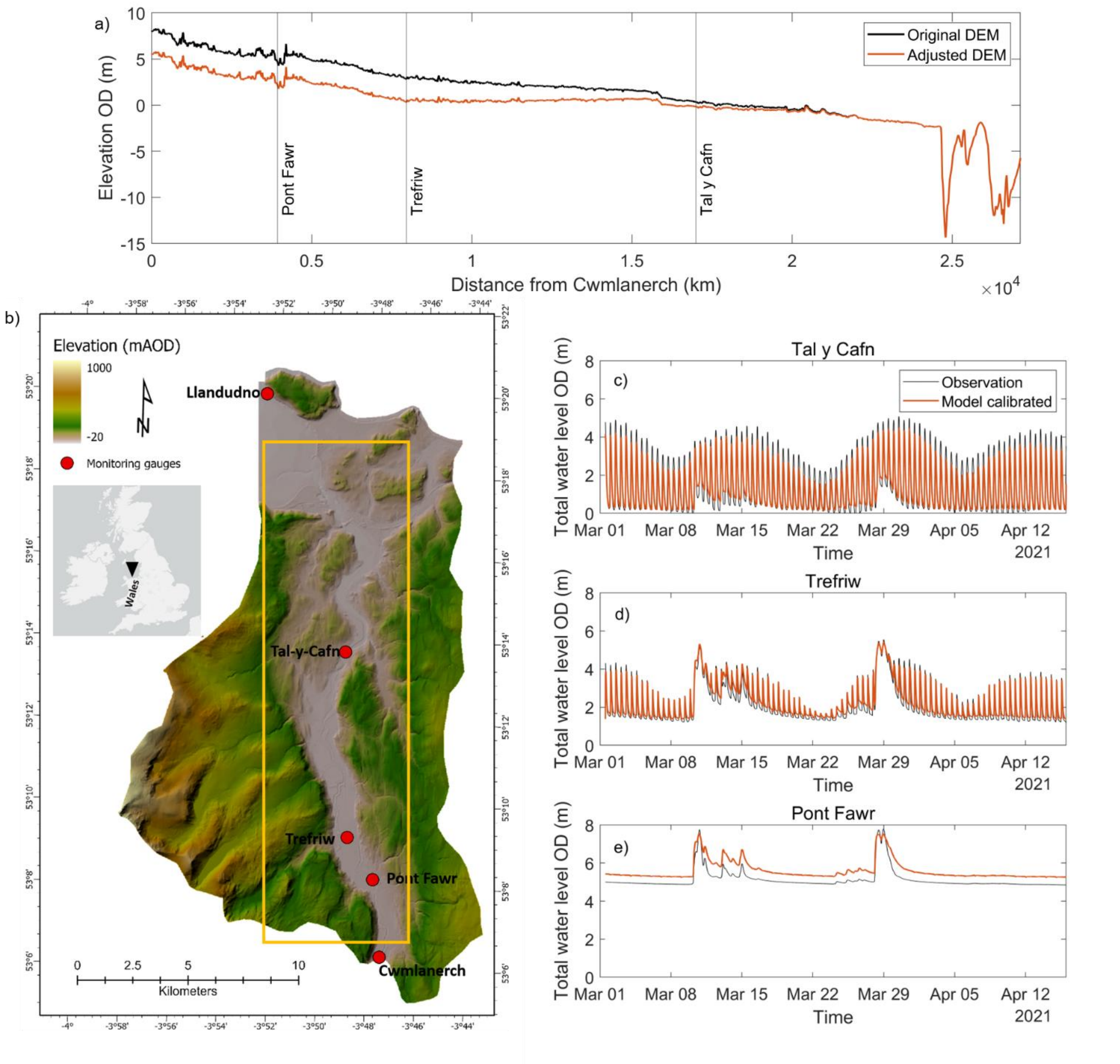

Figure 4 a) Calibrated Conwy estuary model domain showing elevations relative to Ordnance Datum and location of monitoring gauges. The region of interest in the estuary is shown (orange box, size 3920 × 19580 m); b) Longitudinal profile along the channel centreline showing the original elevation derived from the Lidar DTM (black), and adjusted

elevation (red). Comparison between observed (black) and simulated (red) time-series of water levels are shown at c) Pont Fawr, d) Trefriw, and e) Tal-y-Cafn.

2.5 Idealised boundary conditions for model scenarios

The idealised model scenarios were used to add more detail to the historic records of flooding and instrumental data (Figures 2 and 3) to enable driver thresholds for flooding to be established. Three scenarios, each consisting of 520 simulations, tested the influence of the relative drivers of estuary flooding (tidal water level, storm surge, river discharge, and time lag) – see Table 2 and Figure 5. The simulations consisted of 40 river discharge conditions with incrementally increasing *Qmax*, in combination with: (Scenario-1) 13 incrementally increasing tide levels combined with a maximum storm surge; (Scenario-2) 13 incrementally increasing tide levels combined with a mean storm surge; and (Scenario-3) 13 incrementally increasing tide levels combined with a maximum storm surge and a three-hour time lag. In total, 40 (*Qmax*) × 13 (*TWLmax*) × 3 (scenarios) = 1,560 discrete simulations were performed. Each simulation was run for a period of 72 hours, allowing for model spin-up (thus allowing the assumed initial condition to become consistent with the hydrodynamic system) and with *TWLmax* and *Qmax* occurring after ~40 hours. These boundary conditions are described in more detail below.

2.5.1 River discharge

The following method was undertaken to generate 40 idealised discharge time series parameterised on the hydrology of the Conwy. Firstly, a two-parameter gamma distribution was used to generate a synthetic series of normalised, idealised gamma curves, that represent hydrograph shapes that cover the natural range of river flow behaviours experienced in the Conwy based on 30 years of river discharge data from the Cwmlanerch river gauge (see Robins et al., 2018). The gamma curve with the gradient of the rising hydrograph limb that most closely resembled the average gradient of the top 50 *Qmax* events analysed in this study was selected. The selected idealised hydrograph had the largest gradient representing the flashiest flow behaviour. The magnitude of the idealised hydrograph was then scaled to a peak discharge *Qmax* of 25 m^3/s (i.e., a relatively small river flow event that will not likely cause flooding), with a base flow of 20 m^3/s which represents mean flow conditions. The scaling of *Qmax* was successively increased from 25 m^3/s, in 25 m^3/s increments, up to a *Qmax* of 1000 m^3/s (i.e., slightly greater than the maximum recorded event of 901 m^3/s), always keeping a base flow of 20 m^3/s). This created a realistic range of 40 river discharge event time series that were applied to all three scenarios. For each simulation, *Qmax* occurred at 40 hours (Figure 5).

2.5.2 Total water level

The boundary conditions for total water level consisted of 13 time series for each of the three scenarios. These time series were created using idealised tidal signals combined with residual surges. Firstly, a sinusoidal elevation with a period of 12.42 hours (equivalent to the dominant M2 tidal constituent) was created. This was parameterised to represent mean neap tides at Llandudno. Mean spring and neap tidal amplitudes and high tide levels were determined using a harmonic analysis (T-Tide

(Pawlowicz et al., 2002)), based on 12 months of tide gauge data from Llandudno (2002-2003).A subsequent tidal prediction revealed that mean high water neap tides reach 1.82 m (OD) and mean high water spring tides reach 3.6 m (OD) at . The elevation time series was then reproduced 13 times, each time successively increasing the amplitude so that high water was incrementally increased by 25 cm until equivalent to spring high tides. This experimental design purposely neglected the influence of other constituents so that the results were standardised. The model simulated the shallow water propagation of the tide advancing up the estuary.

Secondly, for each of the three scenarios, a residual surge was added to the 13 elevation time series to represent the meteorological contribution to the total water level. The shape of the surge was representative of typical storm conditions for Llandudno (Environment Agency, 2016), as shown in Figure 5. The surge was shifted in time so that the maximum surge height coincided with the fourth high tide (at around 40 hours). For Scenario-1 and Scenario-3, the surge was scaled to the magnitude of the maximum observed skew surge (1.03 m). The resultant 72-hour time series represented several tidal cycles where flooding was not expected (tide-only), followed by a tide + surge event at ~40 hours (where the peak water level is denoted as *TWLmax*), before the regular tidal cycles resumed (Figure 5a and 5c). For Scenario-2, the procedure was repeated, this time by applying a mean observed skew surge (0.13 m) to the predicted tide series (Figure 5b).

2.5.3 Time lag

The timing of *Qmax* relative to *TWLmax* is a key factor in determining compound flooding hazards. This time lag was therefore considered in our sensitivity framework. From the 30-year Cwmlanerch discharge record, we calculated the distribution of time lags (following the method of Lyddon et al., 2021), as shown in Figure 5d. Peaks in river discharge most commonly occurred 0-4 hours before peaks in total water level, i.e., on the rising tide. Initially (Scenario-1 and Scenario-2), we implemented the most common time lag of 0 hours (i.e., both *Qmax* and *TWLmax* were at 40 hours as shown in Figure 5a (Scenario-1) and Figure 5b (Scenario-2). Next, a –3 hour time lag was implemented as shown in Figure 5c, since this was the next most common time lag (Figure 5d), and applied to the 13 tidal + maximum surge time series and 40 discharge time series (collectively named Scenario-3). In total, 13 (*TWLmax*) × 40 (*Qmax*) × 3 (scenarios) = 1560 simulations of 72-hour duration were computed, as summarised in Table 2 and Figure 5.

Table 2: Summary of model scenarios, each containing 520 combination simulations

Set of 520 combination simulations	Peak total water level (*TWLmax*)	River (*Qmax*)	Time lag
Scenario-1	(Neap : 25cm : spring) + max surge = 1.03 m	25 : 25 : 1000 m^3/s	0 hours
Scenario-2	(Neap : 25cm : spring) + mean surge = 0.13 m	25 : 25 : 1000 m^3/s	0 hours
Scenario-3	(Neap : 25cm : spring) + max surge = 1.03 m	25 : 25 : 1000 m^3/s	–3 hours

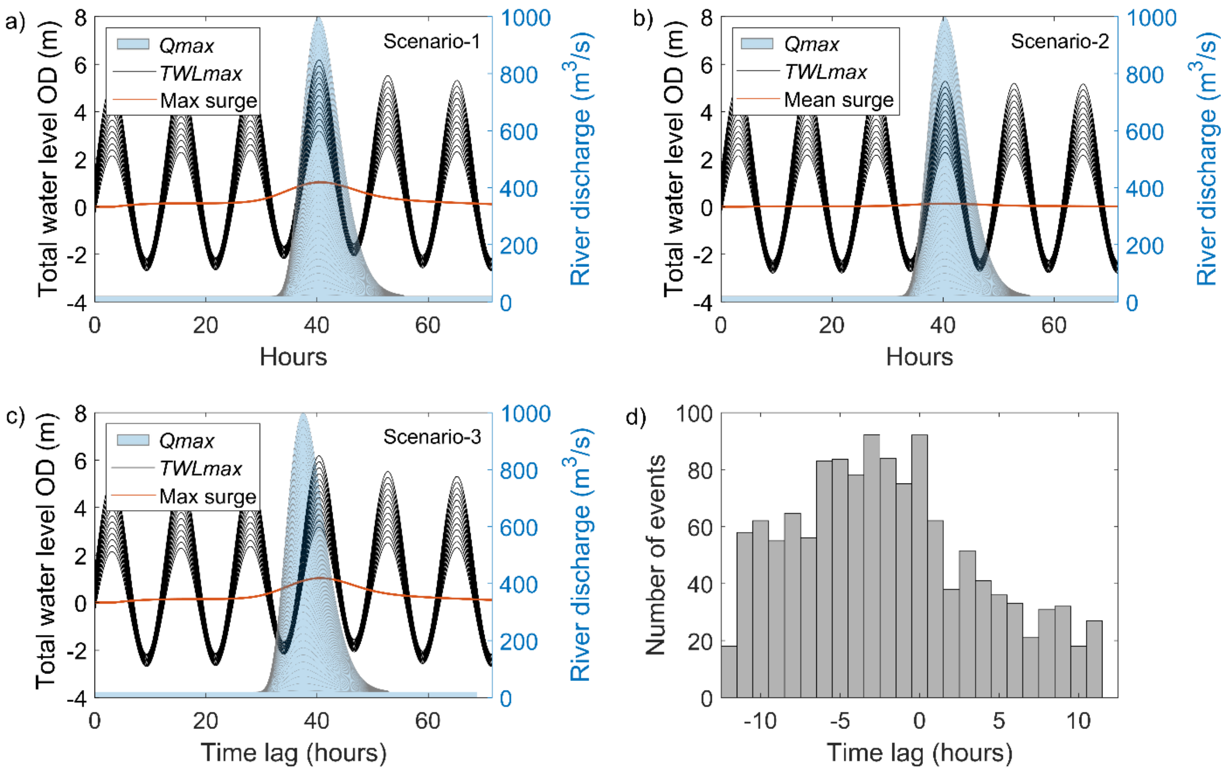

Figure 5: Idealised model boundary conditions for a) Scenario-1, b) Scenario-2, and c) Scenario-3. Sea levels comprised a) tidal + maximum surge with 0 hour time lag (at ~40 hours); b) tidal + mean surge with 0 hour time lag; c) tidal + maximum surge with –3 hour time lag. Each scenario in (a-c) also shows 40 river discharge hydrographs with baseflow of 20 m^3/s and each with a successively increased river flow event with *Qmax* occurring at ~40 hours. d) Histogram of

recorded time lag values between all *Qmax* at Cwmlanerch and *TWLmax* at Llandudno, spanning the period 1980-2023.

2.6 Simulations of flooding

The following methodology was applied to identify the extent of flood extent under each scenario generated in section 2.5. The flooding problem can be represented as a function:

$$FloodArea = f(Qmax, TWLmax, SurgeHeight, Time\ Lag) \quad (1)$$

Where the *FloodArea* quantifies the inundation area (km^2) of the Conwy estuary floodplains, as a function of *Qmax* (25 - 1000 m^3/s), *TWLmax* (tidal + surge) (2.25 - 6 m), surge height (max = 1.03 m, mean = 0.13 m), and time lag (0, –3 hours), as specified in Equation 1.

A high-performance computing system, Supercomputing Wales (https://www.supercomputing.wales/), was used to efficiently run the Caesar-Lisflood solver. The system is capable of handling multiple concurrent computing tasks, to allow the parameter space to be partitioned into 'job blocks'. Blocks were submitted to the system using the SLURM (https://slurm.schedmd.com/) workload manager for batch processing. A typical 72-hour simulation took 1.2 – 2 hours of CPU runtime (on four Intel Xeon(R) cores operating at 2.1 GHz). Overtopping of levees and shallow flows over floodplains can lengthen the computational time, while dry parts of the catchment do not affect the computing time.

The output data comprises water depth grids in time layers with an interval of 15 minutes. Only data of time layers between 2300 and 3500 mins (~38-58 hours), corresponding to the period of widest flooding extents, were stored to reduce space. Post-processing to summarise outputs and calculate *FloodArea* was completed remotely to reduce the transfer load from the nodes to the local computer.

2.7 Scenario analysis

An initial baseline 'no flooding' simulation was performed, from which to calculate *FloodArea* in all subsequent simulations. The baseline simulation represented moderate river flow and sea level conditions whereby water was contained within the main channel, with dry floodplains, and high water levels submerged mid-channel shoals. The baseline was drawn from an actual event in 27-Jan-2016, in which no inundation occurred. This case approximates the Scenario-1 simulation [Q_1TWL_3] (i.e., *Qmax* = 25 m^3/s, *TWLmax* = 3.7 m). A mask has been used to define the region of interest (ROI), see Figure 1a, an area of 196 × 979 cells or ~7.7 km^2, which encompasses the estuary floodplains from the tidal limit at Cwmlanerch to the Conwy Tunnel near the estuary mouth. Six mid-channel shoals were excluded with areas ranging from 0.003 km^2 to 0.17 km^2. The baseline scenario comprises 13,982 wet cells in this ROI (~5.59 km^2). For each simulation, the maximum total flooded area in the ROI was recorded, from which the baseline 'no flood' wet area was subtracted to create the simulated *FloodArea*. A floodplain model cell was considered to have flooded when the local water level exceeded a threshold of 2.5 cm. Wetted surfaces need some time to drain, hence the variation in flooded areas lags behind the water level variations. Furthermore, the minima of the flooded areas do not fully develop before the next flooding phase occurs. As experimented with a number of scenarios accompanying the study, if the depth threshold was set as zero, any thin layer of water is considered inundation, and then the flooded area is monotonically increasing (not shown here). Once the land is wet there is no way to change back into dry. Only new events with higher water levels may expand the inundated area. This is a practical decision, but we also realise that the flooding area is relatively insensitive when this depth threshold varies from 2.5 cm to 12.5 cm. The *FloodArea* for each simulation was the inundated area exceeding this threshold. *FloodArea* and absolute difference in *FloodArea* (between scenarios) are presented throughout the 520-simulation parameter space for each of the Scenarios-1-3.

Spatial inundation maps were presented. Four cases were presented in this way, based on the Scenario-3 simulations: (i) TWL dominated flooding; (ii) Q dominated flooding; (iii) moderate compound flooding, and (iv) extreme combined flooding. Spatial variability in flooding was also presented as variations in lateral flood extent (in m) across east-west transects of the floodplains at regular 20 m intervals, from the estuary mouth to the tidal limit – done this way since the Conwy is almost aligned in the north-south direction (typical deviation in angle of ±30°). Again, the four cases (i-iv) above were presented in this way for lateral flood extent, based on the Scenario-3 simulations. For each case (i-iv), three simulations were presented with similar *FloodArea*: (i) TWL dominated, 3.1-6.5 km^2, (ii) Q dominated, 11.13-11.8 km^2, (iii) moderate compound, 5.4-8.3 km^2, and (iv) extreme compound, 8.8-9.1 km^2.

2.8 Estimating joint probabilities

Joint probabilities are important in statistics, providing a way to model and analyse the simultaneous occurrence of events. In the context of flood analysing, the joint probabilities identify the likelihood of combinations of coastal and river conditions occurring, and capture relationships between variables (Wu et al., 2021; Olbert et al., 2023; Moradian et al., 2023). The joint probability of river and sea level conditions can be interpreted in the context of i) hydrodynamic model outputs to identify the likelihood of combinations of conditions occurring to create a flood hazard, and ii) recorded historic flood events to provide context to the severity of flood events. Copulas are effective at modelling nonlinear dependence structures and joint distribution between two variables. The copulas functions (Sklar, 1959) are used here to generate synthetic bivariate pairs of extreme sea levels and river discharges, thus making their respective probability distribution more robust to apply joint probability methods. The Copula method was employed in this study to compute joint probabilities for extreme sea levels and river flows co-occurring in the Conwy for the first time. The joint probabilities were computed using the framework introduced by Sadegh et al. (2017) and Moradian et al. (2023). The proposed framework uses three main components: (i) 16 statistical distributions were employed to identify the best marginal distributions; (ii) 26 distinct Copula functions were applied to sea level and river flows; and (iii) the Bayesian method was employed to compute the joint probabilities. The following sections provide a concise overview of the steps involved in this framework, while more comprehensive details can be found in Sadegh et al. (2017, 2018), Yazdandoost et al. (2020), and Moradian et al. (2023).

2.8.1 Statistical marginal distributions

To identify the most suitable marginal distributions for the data, researchers commonly employ parametric or nonparametric distributions. It is important to note that each variable's marginal distribution is modelled using the best-fitted distribution, as shown in Table 6 of Moradian et al. (2023). To assess the accuracy of the marginal distributions, their significance at a 5% level is evaluated using the Chi-square goodness of fit test (Greenwood and Nikulin, 1996). Furthermore, various metrics are used for statistical evaluations, as detailed in Table 5 of Moradian et al. (2023). These metrics include the Akaike information criterion (AIC), Bayesian information criterion (BIC), Maximum likelihood estimation (MLE), Nash-Sutcliffe efficiency (NSE), and Root mean square error (RMSE).

2.8.2 The Copula Method

Copula functions are mathematical functions that link or connect time-independent variables (Nelsen, 2007), irrespective of their individual distribution characteristics (Genest and Favre, 2007). According to Sklar's theorem (Sklar, 1959), if we have two continuous random variables X and Y with probability density functions of $f_x(x)$ and $f_y(y)$, and cumulative distribution functions of $F_x(x)$ and $F(x)$, respectively, and if both and have the same marginal distribution function F, then there exists a unique Copula function: C: $[0.1]^2 \rightarrow [0.1]$ which serves as a bivariate cumulative distribution function and has uniform margins:

$$F\ (x, y)\ =\ C(F_x(x), (F_x(y)) \qquad (2)$$

In an n-dimensional space, the cumulative distribution function F can be defined in terms of the Copula function C and the marginal distribution functions as follows:

$$F\ (x_1, x_2, \ldots, x_n)\ \ =\ C(F_1(x_1), F_2(x_2), \ldots, F_n(x_n)) \qquad (3)$$

where $F_1, F_2, \ldots, F_n$ are the marginal distribution functions (Nelsen, 2007).

A wide range of Copula functions are available, categorised into various families such as Gaussian, Plackett, Archimedean, elliptical, and t families (Abbasian et al., 2015). Table 4 in Moradian et al. (2023) provides a compilation of the applied 26 Copula families and their corresponding mathematical descriptions. Here, to choose the best Copula family, different metrics were used according to Table 5 in Moradian et al. (2023). In addition, the correlation coefficients for the used flood pairs are

Pearson's Linear Correlation Coefficient, Kendall's-Tau Correlation Coefficient and Spearman's Rho Correlation Coefficient (Akoglu, 2018).
The statistical method entails assessing the likelihood of an event, taking into account existing knowledge of conditions that may be associated with the occurrence of the event. The concept has demonstrated remarkable success in diverse fields, including hydrology (Sadegh et al., 2017) and weather forecasting (Khajehei et al., 2017; Yazdandoost et al., 2020).

3 Results

Results are presented for simulated *FloodArea* for Scenarios-1-3 in the Conwy estuary (Sections 3.1 - 3.3), where a range of 1560 idealised simulations represent likely sea level and river flow 'compound storm events' that could lead to flooding. Next (Section 3.4), for Scenario-3, a selection of simulated flooding maps and along-channel flooded width graphs are presented. Finally (Section 3.5), joint probabilities are assigned to the compound flood drivers.

3.1 Scenario-1 [tide series + max surge combined with river discharge series and 0 hour lag]:

For Scenario-1, a surge tide event (skew surge = 1.03 m) was simulated, with a 0-hour time lag (i.e., *Qmax* and *TWLmax* occurred simultaneously at 40 hours of the 72-hour simulations). The simulated *FloodArea* (km^2) for all 520 simulations is shown in Figure 6 where white represents little to no flooding, and red indicates maximum flood extent (> 10 km^2). The top 50 *Qmax* and *TWLmax* events, and the recorded flooding events, are also shown. As expected, there was no or little (< 1 km^2) flooding simulated under the low-magnitude river flow and sea level events (*Qmax* < 100 m^3/s and *TWLmax* < 4 m). Flooding wasn't simulated with *Qmax* of 25 m^3/s until *TWLmax* was 3.95 m, and then as *Qmax* was increased a reduced *TWLmax* was needed to cause flooding. For example, flooding was simulated with *Qmax* = 50 m^3/s and *TWLmax* = 3.6 m, as well as *Qmax* = 100 m^3/s and *TWLmax* = 3.4 m. *FloodArea* increased as *Qmax* and *TWLmax* increased. The simulated maximum *FloodArea* was 11.2 km^2 under the *Qmax* = 1000 m^3/s and *TWLmax* = 10 m combination.

The contours shown in Figure 6 connect the model simulations with similar *FloodArea* (although not necessarily inundation of the same areas within the floodplains) and suggest a complex relationship between *Qmax* and *TWLmax* drivers in terms of simulated flooding. The contour gradients, shapes, and separation can therefore be interpreted to explain the dynamics of flooding. The contour gradients change across the range of simulations as *FloodArea* becomes more or less sensitive to one driver or the other. The 1 and 2 km^2 contours are broadly straight diagonals (bottom left part of Figure 6), as are the 9, 10 and 11 km^2 contours (top right part of Figure 6). In these cases, *FloodArea* is broadly equally sensitive to both *Qmax* and *TWLmax* drivers. Convex contours (e.g. the middle sections of the 3 and 4 km^2 contours in Figure 6) indicate a compounding flood effect, as the addition of both drivers amplifies *FloodArea*. Conversely, concave contours (e.g. the middle sections of the 5-7 km^2 contours in Figure 6) indicate a degressive flooding effect, where the combination of the drivers leads to relatively less *FloodArea*. There is a widening between the convex (4 km^2) and concave (5 km^2) contours in the centre of Figure 6, indicating that simulated flooding was relatively insensitive to changes in *Qmax* between 350 and 500 m^3/s and *TWLmax* between 4 and 5 m. Hence, several simulated compound event permutations within these driver ranges produced broadly similar *FloodArea*. Contours that are near horizontal (e.g. the 5 and 6 km^2 contours in the top left and middle parts of Figure 6) indicate that changes in flooding are predominantly driven by changes in *TWLmax*. Whereas contours that are near vertical (e.g. the 5 and 6 km^2 contours in the bottom middle part of Figure 6) indicate that changes in flooding are predominantly driven by *Qmax*. Contours that are relatively close together (e.g. 5-7 km^2 contours where *TWLmax* > 5.25 m) potentially indicate key thresholds where small changes in one or both drivers lead to large changes in flooding.

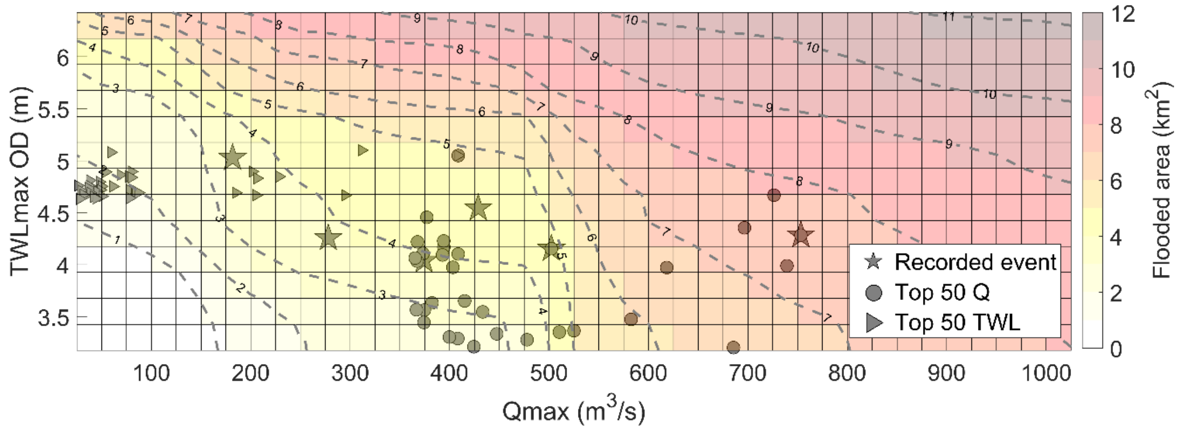

Figure 6: Scenario-1 (13 tide + max surge water levels combined with 40 river flow events, with 0 hr time lag): Coloured surfaces represent modelled *FloodArea* (km^2) from combinations of 520 *Qmax* and *TWLmax* simulations. The contours link common *FloodArea* magnitude. Shapes correspond with Figure 2 and indicate extreme *Qmax* and *TWLmax* values within the historical record (NRW Recorded Flood Events (stars), top 50 *TWLmax* (triangles) and top 50 *Qmax* (circles)).

3.2 Scenario-2 [tide series + mean surge combined with river discharge series and 0 hour lag]:

Scenario-2 simulated the effect on flooding of a mean surge magnitude, in difference to the maximum surge simulated in Scenario-1. The difference from Scenario-1 in simulated *FloodArea* is shown in Figure 7, by subtracting *FloodArea* results of Scenario-2 from Scenario-1. The *TWLmax* boundary conditions were lower for Scenario-2 (2.25-5.25 m) than for Scenario-1 (3.75-6.25 m), due to the smaller contribution of the surge, and gives insight into flooding dynamics under lower *TWLmax* values. Both sets of scenarios have the same underlying M2 tidal signal, so the absolute difference in *FloodArea* is due to the influence of the surge magnitude/shape for each scenario. All Scenario-1 simulations cause a larger *FloodArea* than Scenario-2 simulations, for the same *Qmax* and *TWLmax* values. The influence of the different surge magnitudes/shapes on *FloodArea* has the greatest impact under high *TWLmax* conditions (> 4.25 m), and with *Qmax* values below 500 m^3/s, causing a variance of up to 5 km^2 in *FloodArea*. Under low river and low sea level scenarios (bottom left of grid), or high river and sea level scenarios (top right of grid), a larger surge consistently causes 2-3 km^2 more *FloodArea*.

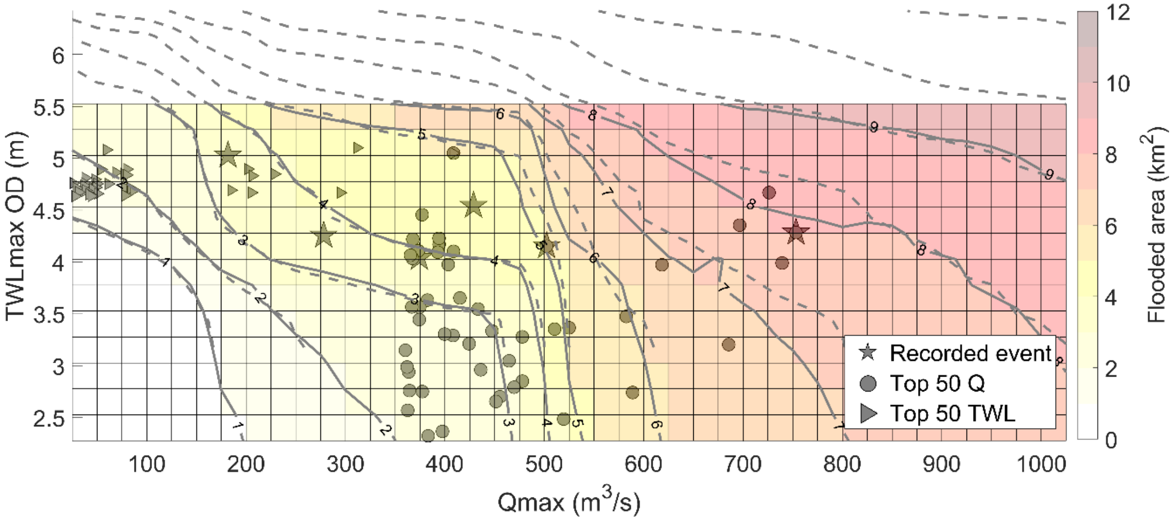

Figure 7: Scenario-2 (13 tide + mean surge water levels combined with 40 river flow events, with 0 hr time lag): Coloured surfaces represent modelled *FloodArea* (km^2) from combinations of 520 *Qmax* and *TWLmax* simulations. The dashed contours link common *FloodArea* magnitude for scenario-2, whereas the solid contours refer to scenario-1 for comparison. Shapes correspond with Figure 2 and indicate extreme *Qmax* and *TWLmax* values within the historical record (NRW Recorded Flood Events (stars), top 50 *TWLmax* (triangles) and top 50 *Qmax* (circles)).

3.3 Scenario-3 [tide series + max surge combined with river discharge series and -3 hour lag]:

Scenario-3 simulated the effect on the flooding of a –3 hour time lag between *Qmax* and *TWLmax*, in difference to the 0 hour time lag simulated in Scenario-1 (both Scenarios simulated a maximum surge event). Differences in *FloodArea* under an assigned –3 hours time lag (i.e. *Qmax* preceding *TWLmax* by 3 hours, hence occurring during flooding tide), compared with Scenario-1, are shown in Figure 8. Generally, a similar trend in flooding was simulated for both Scenarios and the gradients of the *FloodArea* contours were similar (see also Figure S2 in the Supplementary Material). One interesting difference, however, was that lower magnitude drivers (*Qmax* < 200 m^3/s, *TWLmax* < 3 m) simulated a larger *FloodArea* for Scenario-3 than Scenario-1. The *FloodArea* contours in Scenario-3 were smoother in shape than for Scenario-1, most notably on the 5 and 6 km^2 contours. This could indicate a more compounding effect of the drivers with a –3 hour time lag, since the lag causes more of the river water on the rising limb of the hydrograph to be retained within the estuary by the flooding tide. The simulated

FloodArea was sensitive to the shift in time lag however with notable variation depending on simulations. The blue cells in Figure 8 indicate that the –3 hour time lag scenarios produced a greater *FloodArea* than in Scenario-1. The –3 hour time lag had a small influence (generally < 0.5 km^2) on *FloodArea* for *Qmax* < 425 m^3/s across all *TWLmax* simulations. For *Qmax* > 425 m^3/s, the differences in *FloodArea* were generally > 0.5 km^2. The greatest difference in *FloodArea* was 1.2 km^2 from the simulation with *Qmax* = 475 m^3/s and *TWLmax* = 4.7 m. Differences in *FloodArea* > 1 km^2 were also simulated for *Qmax* = 550-650 m^3/s and *TWLmax* < 5 m. For *TWLmax* > 5 m and *Qmax* > 800 m^3/s, *FloodArea* appeared less sensitive to the time lag (differences <0.5 km^2). However, for *TWLmax* < 5 m and *Qmax* > 800 m^3/s, *FloodArea* appeared more sensitive to the time lag (differences of 0.5-1 km^2), presumably because the stronger river discharges were able to counter the blocking effect of weaker tidal currents. Irrespective of the time lag, a *Qmax* of 475-600 m^3/s was again shown as the river conditions where there is a marked change in *FloodArea* and high sensitivity to *Qmax*. A –3 hour time lag produces a 7.7 % increase in flooding across the parameter space compared with Scenario-1; Scenario-1 produced a total of 3299 km^2 *FloodArea*, and Scenario-3 produced 3553 km^2 *FloodArea*.

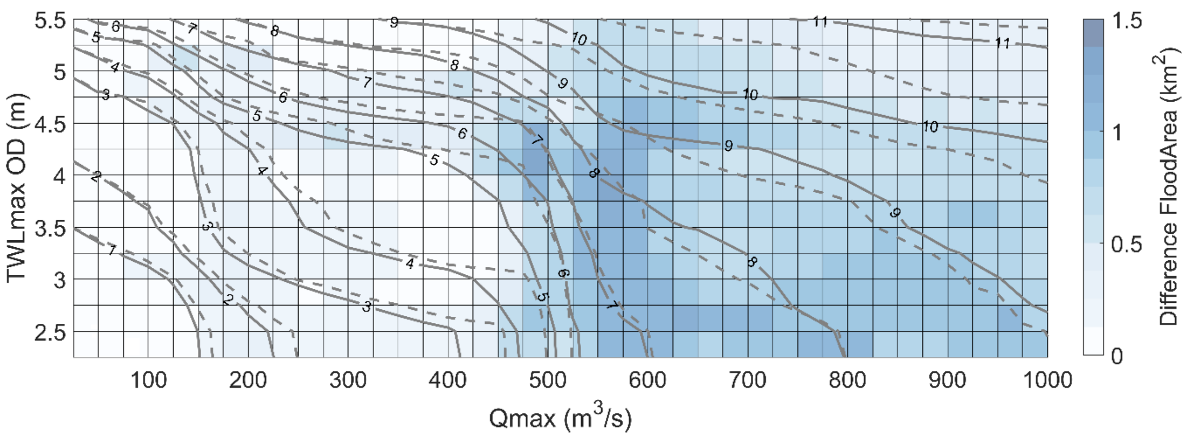

Figure 8: Coloured surface represents the absolute difference in modelled FloodArea between Scenario-1 (maximum surge with 0 hour lag) and Scenario-3 (maximum surge with -3 hour lag). The solid contours link common FloodArea magnitude for scenario-3, whereas the dashed contours refer to scenario-1 for comparison.

3.4 Spatial distribution of the flooded area

Aside from simulating the *FloodArea* considered in Sections 3.1–3.3, it is also important to specify where the simulated flood water is distributed. To quantify the distribution of flooding in various parts of the estuary-catchment system, four cases were considered:

(a) TWL dominated: *TWLmax* ≥ 6.1 m, *Qmax* ≤ 25 m^3/s.

(b) Q dominated: *TWLmax* ≤ 3.1 m, *Qmax* ≥ 1000 m^3/s.

(c) Moderate compound: *TWLmax* 4.7-4.9 m, *Qmax* 475-500 m^3/s.

(d) Extreme combined: *TWLmax* ≥ 6.1 m, *Qmax* ≥ 1000 m^3/s.

Figure 9 shows the spatial distribution of flooding for the above four cases for Scenario-3 (tide + max surge combined with river events and –3 hour time lag). The TWL-dominated event is shown in Figure 9a, where water inundated the lower and middle estuary. The Q-dominated event simulated upstream flooding (Figure 9b). The moderate compound event is shown in Figure 9c where the inundation pattern shows flooding mostly at the upstream region and part of the middle estuary. Finally, the extreme combined event is shown in Figure 9d, where water inundated wide parts of the floodplains throughout the estuary. It can be seen that the flooded region of Figure 9d is broadly the union of that in Figures 9a and 9b.

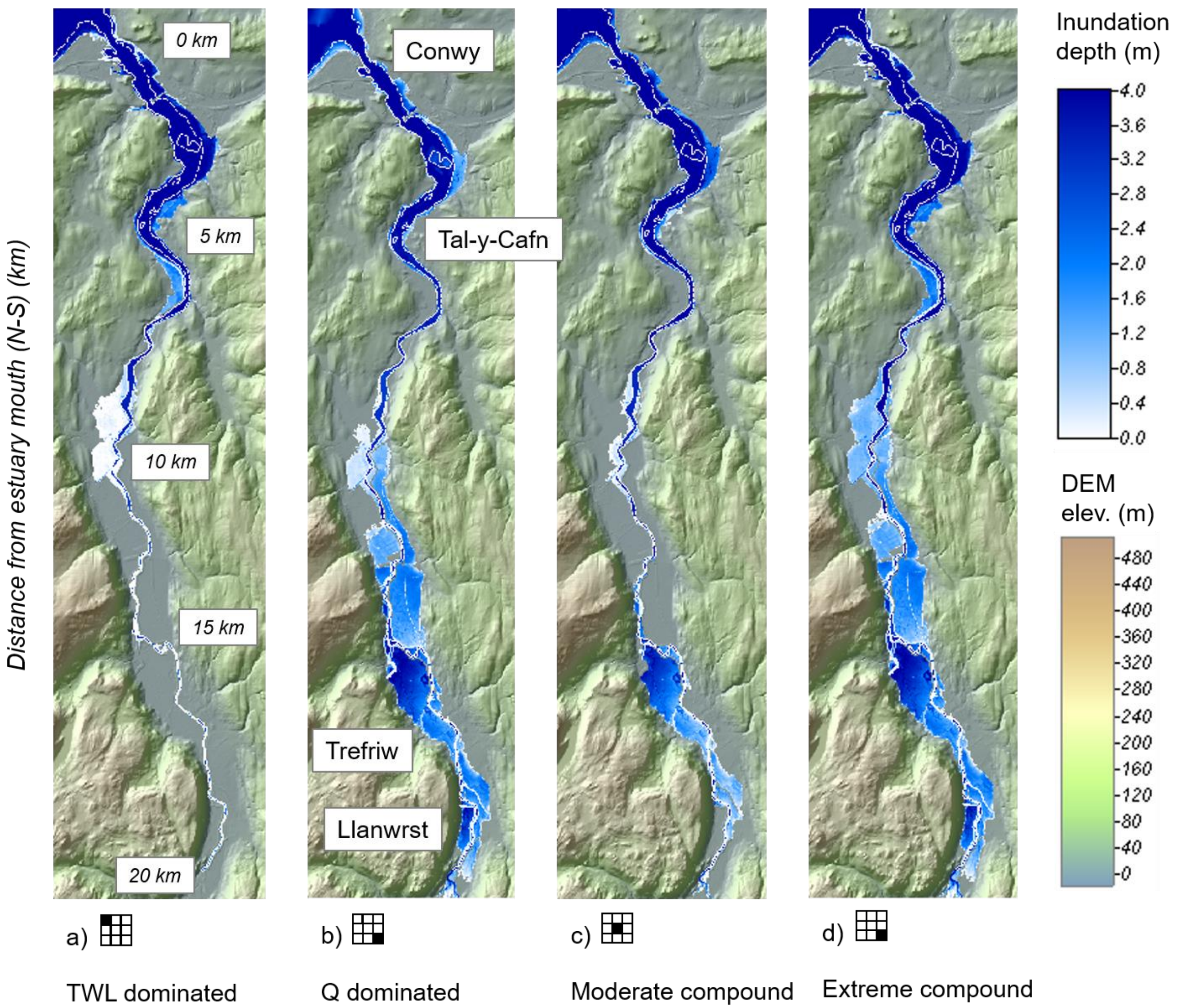

Figure 9: Scenario-3 (tide + max surge with river events and -3 hour lag): Simulated maximum flooded extent (blue shades) of the region of interest for cases: (a) TWL-dominant (Q_1TWL_{13}), (b) Q-dominant ($Q_{40}TWL_1$), (c) Moderate compound ($Q_{20}TWL_7$), (d) Extreme combined ($Q_{40}TWL_{13}$). Corresponding *FloodAreas* are 5.6 km^2, 11.5 km^2, 8.9 km^2, and 6.6 km^2, respectively. The icons show the relative position of each case (a-d) on the *TWLmax:Qmax* parameter space (detailed in Supplementary Information). The white dashed lines delineate the shoreline in the 'no flooding' basecase. The green-brown shading denotes dry land.

The lateral extents of flooding, defined as the width of the inundated area in the direction perpendicular to the river channel, for Scenario-3 for cases (a-d) are presented in Figure 10. In each case (a - d) three adjacent simulations are shown to depict some driver sensitivity. For the TWL dominated case, the three simulations presented in Figure 10a show extensive lateral inundation (15-60 m) simulated along the lower estuary floodplains (distance up to 6 km from the estuary mouth), with limited inundation between 6-8 km, then extensive inundation further up-estuary (8-14 km) that was sensitive to *Qmax* (in the range 25-100 m^3/s), and limited inundation beyond 14 km. For the three Q dominated cases (Figure 10b), extensive inundation (20-60 m) was simulated in the upper estuary (8-19 km) with minimal sensitivity between the three simulations. For the moderate compound event cases (Figure 10c), simulated lateral inundation showed large sensitivity to forcing conditions, with up to 40 m variability between the three simulations at 10-14 km. The capacity of the estuary for floodwater storage is clearly sensitive in this region. Finally, for the extreme combined event cases (Figure 10d), extensive lateral flooding (15-60 m) was simulated throughout the lower and upper estuary, except between 6-8 km where there was again limited flooding simulated. There was little sensitivity (< 1 m) between the three simulations shown.

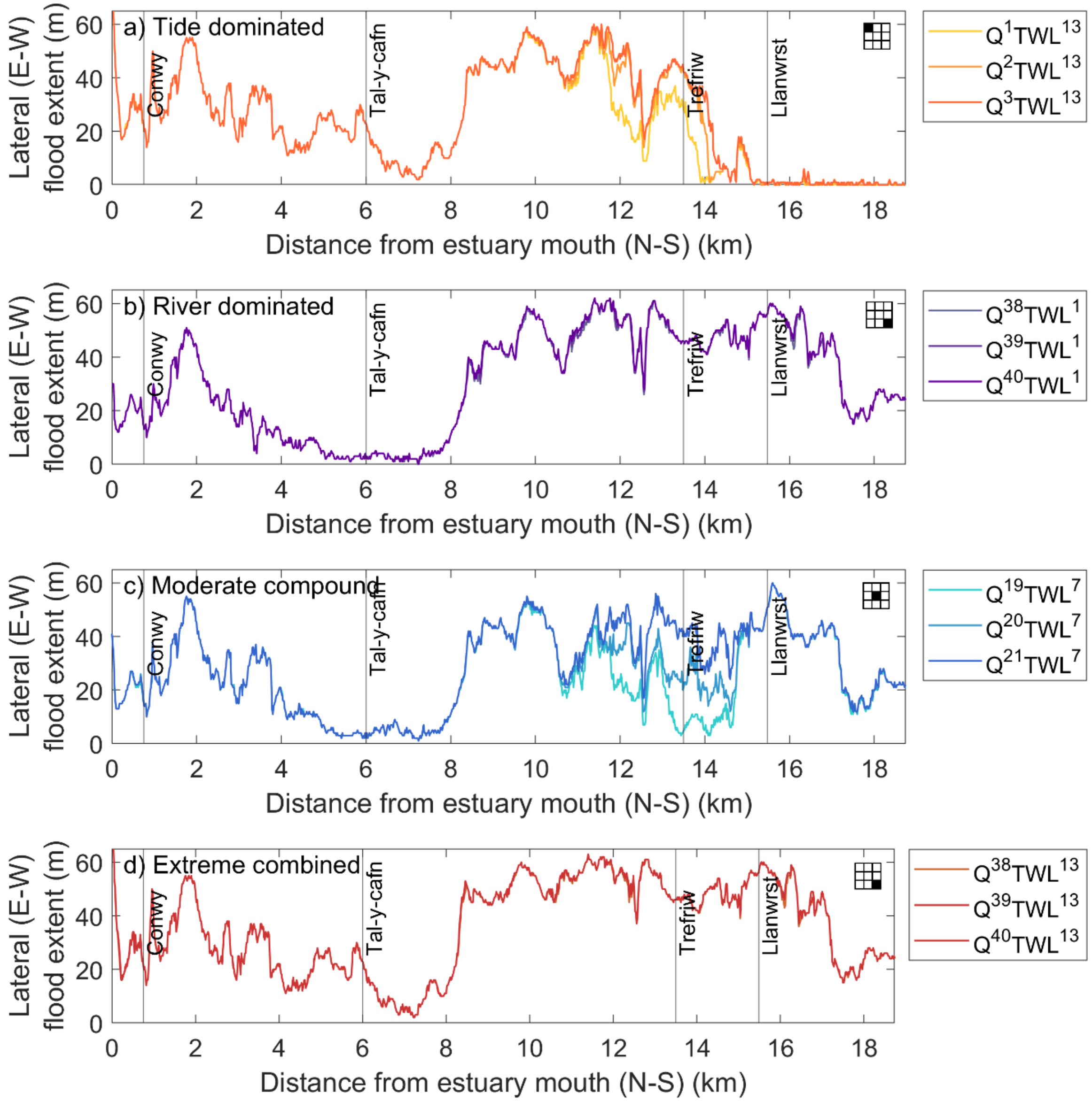

Figure 10: Scenario-3 (tide + max surge with river events and -3 hour lag): Distribution of lateral flooding along the Conwy estuary floodplain for four cases across the *TWLmax:Qmax* parameter space: (a) TWL dominant ($Q_{1\text{-}3}TWL_{13}$); (b) Q dominant ($Q_{38\text{-}40}TWL_{1}$); (c) Moderate compound ($Q_{19\text{-}20}TWL_{7}$); and (d) Extreme combination ($Q_{38\text{-}40}TWL_{13}$). Lateral flooding is measured in the east-west direction. Along-estuary distance is measured in the north-south direction

(from the estuary mouth to upstream). For each case (a-d), three simulations are presented (constant *TWLmax* and varying *Qmax* - see also Figure S3). The icons show the relative position of each case (a-d) on the *TWLmax:Qmax* parameter space (detailed in Supplementary Information).

3.5 Assigning probability to flood drivers

Figure 11 shows joint probabilities calculated from observed total water level at Llandudno and river discharge at Cwmlanerch, presented on the *TWLmax:Qmax* parameter space and overlaying the distribution of extreme events in the historic record. Figure 11 represents a novel approach to interpreting joint probabilities in the context of historic storm events, to better understand the relationship between drivers and impacts of flooding. The joint probabilities highlight the likelihoods and severities of the historic extreme compound events. There were seven historic events which have a probability of <0.01, indicating less than 1 event in 100 years of this magnitude, six of which are recorded as causing flooding (yellow circles), whereas for one of these events no flooding was recorded (blue triangle). The no flooding event was 10 February 1997; *Qmax* was 311 m^3/s which peaked 1 hour 30 minutes before *TWLmax*, recorded as 5.1 m, including a 0.48 m skew surge. Reports indicate this was a high water level event, associated with a 5 year sea-level return period, but these conditions did not cause flooding or no flooding was recorded (HR Wallingford, 2008). This method allows return periods to be assigned to historic extreme events and recorded flood events, and to estimate the likelihood and severity of potential future events. Figure 11 shows that the same joint probability can occur from a range of combinations of *Qmax* and *TWLmax* conditions. For instance, an event with a 0.2 exceedance probability (1 event in 5 years) can occur on a TWL dominated, Q dominated, or moderate compound event.

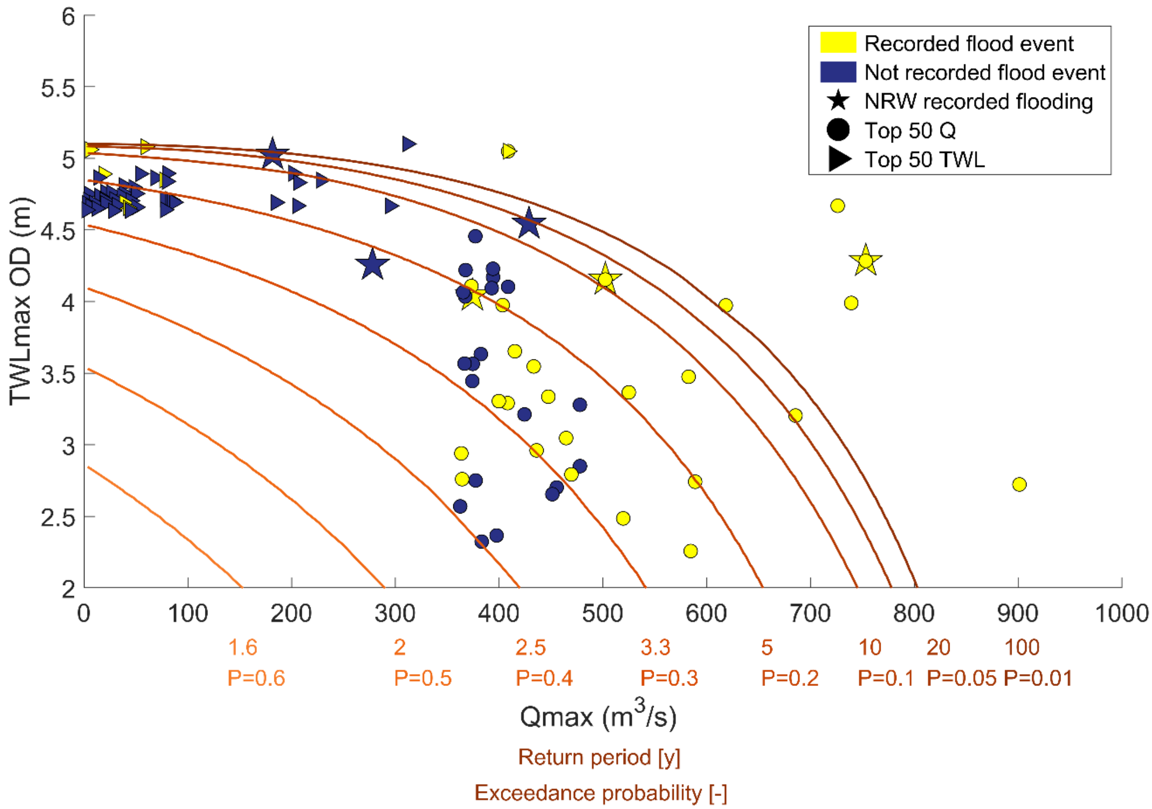

Figure 11: Joint probabilities for *TWLmax* and *Qmax* in the Conwy Estuary, where P = exceedance probability, ranging from high likelihood of co-occurrence (P=0.6) to low likelihood of co-occurrence (P=0.01) overlaid the distribution of extreme events (recorded and not recorded flooding) in the historic record.

4 Discussion

This research has established site-specific driver-thresholds for flooding in an estuary environment, using hydrodynamic modelling. The simulations have been verified and contextualised using documented records of flooding, together with data analysis and statistical analysis of instrumental gauge time series. With application to the Conwy estuary, N-Wales, the hydrodynamic inundation model was applied to a series of idealised combined river and sea level compound events. We show that flooding is co-dependent on *TWLmax*, *Qmax*, and their relative time lag, and that historic records of flooding can be used to set driver and flood extent thresholds that isolate minor and severe flooding. Below, we discuss the thresholds of flooding and the importance of accurate records of historic flooding events. We consider these thresholds may change under different driver behaviours and combinations, and future climate conditions.

4.1 Thresholds for flooding

Since there are multiple drivers of flooding in estuaries, single-value driver-thresholds cannot be used, e.g., for the Conwy estuary we show for the first time that flooding is co-dependent on *TWLmax*, *Qmax*, and their relative time lag. The simulated flooding presented in Section 3 shows the total inundation (*FloodArea*) across the estuary system and includes both minor or nuisance flooding up to severe flooding. Recorded events of flooding are isolated based on time lag and associated web scraped tag(s) (cf. Section 2.3), and presented with *FloodArea* contours from Scenario-3 to identify if there is a simulated *FloodArea* threshold that matches the recorded flooding events (Figure 12). The 2 or 3 km^2 contour lines can be interpreted as a minimum *FloodArea* contour for recorded flooding in the Conwy. The coastal events (Figure 12c) occur under high sea level and across a range of river discharge combinations, indicating thresholds for flooding in the coastal zone should consider sea level as the dominant driver.

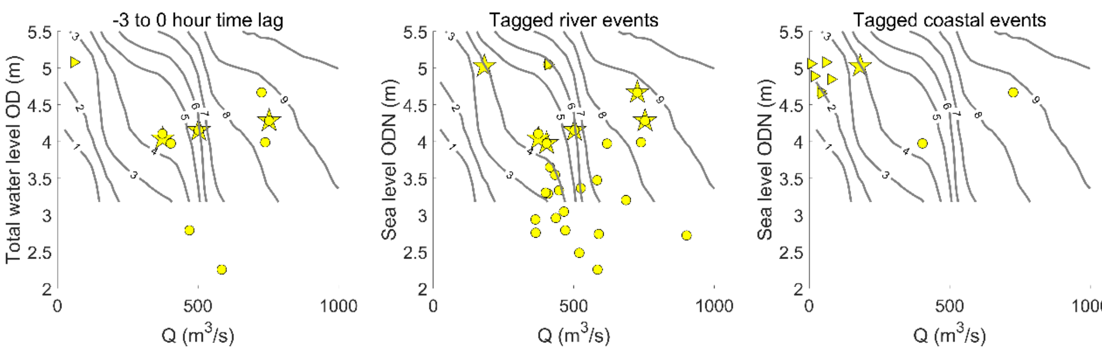

Figure 12: Recorded flood events with a) a time lag between 0 to -3 hours; b) with tag [1] for river event; c) with web-scraped keywords (tags) [3 4] for coastal event, all presented with *FloodArea* contours from scenario-3.

Whilst the *FloodArea* representation gives a good overall perspective of flooding dynamics, a different approach is needed to establish co-dependent driver-thresholds for flooding at different locations within the estuary. For a chosen location, as a first step, a flood-threshold (i.e., depth of inundation) has to be established. For instance, one might expect to assign a different flood-threshold for an area of unused woodland than an agricultural field or a dwelling or road, based on socio-economic impact metrics (Cutter et al., 2013; Alfieri et al., 2016). Next, the inundation modelling shown in Section 3 can be used to predict whether flooding is likely to have occurred or not for the range of compound events within the parameter space, and hence define the site-specific co-dependent driver-thresholds. This is an approach often used for coastal infrastructure, including nuclear sites (e.g. ONR, 2021) but rarely extended to individual properties or land users. We have demonstrated this procedure below for four discrete locations within the Conwy estuary floodplains: (i) primary school, Conwy, (ii) farmland, mid-estuary; (iii) section of railway, mid-estuary; and (iv) dwelling, Llanwrst. We used Scenario-3 (tide + max surge combined with river events with a –3 hour time lag) for this demonstration since this scenario predicted the most flooding. Figure 13 shows the co-dependent driver-thresholds for each location (i-iv). Figure 13 shows TWL dominated flooding in the lower estuary when sea level > 5.7 m at the school and > 4.9 m at farmland, and river dominated flooding in the upper estuary at dwellings when river discharge > 750 m^3/s. This also aligns with what is shown in Figure 10, and single variable (Q *or* TWL, respectively) flood probability analysis may be appropriate in these locations. Moderate compound flooding in the mid-estuary shows flooding under a wider range of TWL and Q combinations, and shows that joint probability analysis is necessary when both drivers influence flood magnitude.

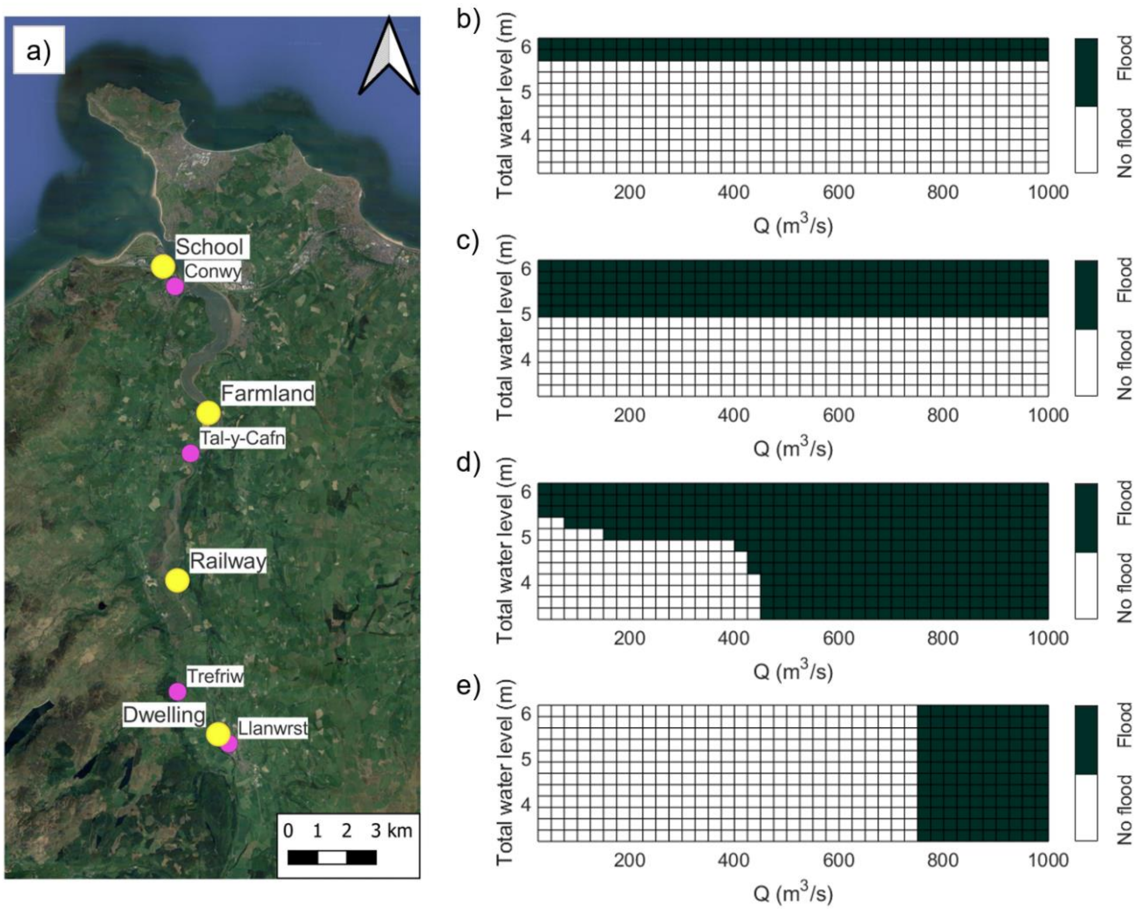

Figure 13: Site-specific flood thresholds to show the conditions that cause flooding to occur or not within the Conwy Estuary (a) using model outputs from Scenario-3 at: (b) primary school in lower estuary; (c) farmland in lower estuary; (d) railway in mid estuary; and (e) dwelling in upper estuary. Figure 13a Basemap © OpenStreetMap 2023

4.1.1 Flood dynamics related to driver magnitude & timing

We show that flood forecasts need to be sensitive to both fluvial and sea level drivers of flooding in the Conwy Estuary, N-Wales, particularly under medium levels (45-60th percentiles) of river discharge and total water level. Flood hazard assessments must consider a bivariate approach to both river discharge and sea levels across an estuary, otherwise univariate approaches will not appropriately characterise the hazard and will underestimate compounding effects (Moftakhari et al., 2017). Combined river and sea level simulations show that when the drivers are extreme (e.g. > 85th percentile), they act equally and consistently produce the highest magnitudes of flood inundation irrespective of their relative timing. The volume of riverine freshwater is the dominant driver contributing to high water levels in the estuary. This could be evidence of the backwater effect, where high river discharge can push back low levels of tidal water, resulting in a temporary increase in water levels within the estuary (Ikeuchi et al., 2015; Feng et al. 2022).

Results show that flood forecasts need to be particularly accurate for Conwy Estuary when the river discharge is between 450-550 m^3/s, which represents moderate conditions. We show that within this range of discharge there is considerable variability in flood inundation across a range of sea-level magnitudes, and also sensitive to the timing of *Qmax* relative to *TWLmax*. This critical range of discharge values, between 450 - 550 m^3/s, could be related to the holding capacity of the estuary as there may be storage volume for flood water below these magnitudes of discharge. This critical range of discharge values also represents a threshold for a change in the behaviour of the drivers. Analysis of *FloodArea* contour shapes/gradients superimposed on historic flood inundation records shows that compound effects are most significant under medium levels of river discharge and sea level. Below these medium levels, then one or the other driver is more dominant. Above this level, then both drivers are equally dominant in their contribution to flooding. These insights show that both drivers must be considered as dependent and interacting in flood forecasts, to ensure that compound flood effects are captured and planned for.

An analytical model has been used in an idealised, meso-tidal estuary to show that there is always a point where river discharge effects on water level outweigh tide-surge effects (Familkhalli et al., 2022). Non-linear effects and interactions between sea level and river discharge can influence compound effects, including tidal damping, and tidal blocking, influence the location at which river flow effects are larger than marine effects, or vice versa (Cai, 2014; Hoitnik and Jay, 2016; Xiao, 2021). The magnitudes at which river discharge and sea level will cause compound effects to amplify flood inundation will vary between estuaries. These effects may not occur in some estuaries, and be more extreme in others (Harrison et al., 2022). It is likely that a range of factors will control this including tidal range, substrate type and bed friction, coastline aspect, estuary geometry and size, catchment size, type and geology, river network, river transmission times, prevailing weather conditions, antecedent weather, and local climate (Familkhalli et al., 2022). The parameter space could be developed by considering additional hydrograph time lags, and exploring the timing of the surge relative to tidal high water which could influence the magnitude and volume of the total water level (Lyddon et al., 2018; Khanam et al., 2021). The lag time is currently presented as between *Qmax* and *TWLmax*, however there could be asymmetries within the estuary that prevent tidal slack water occurring at *TWLmax*. The *Qmax* lag relative to slack tide (e.g. turning from flood to ebb) could be explored, however significant 3D lateral flows in the Conwy Estuary (e.g. Robins et al., 2012; Howlett et al., 2015) would mean that identifying location and timing of slack water would require a 3D baroclinic model. These additional parameters could alter the position, shape, or angle of threshold contours, , or understanding of flood dynamics. A better understanding of estuarine thresholds can enhance how managers and engineers plan coastal protection strategies, including where to place defences, infrastructure, and buildings.

4.1 Documented records of flooding

Historical records of flooding in the Conwy estuary are incomplete, with few flooding events pre-2004 documented and available online. More recent flooding events have only been recorded online unsystematically and are contingent on the severity of the impact, suggesting that smaller flooding events or flooding away from people and infrastructure have potentially been undocumented. Additionally, documented flooding events tend to focus on the impacts rather than the drivers that caused the hazard. This study adds to the historical catalogue of flooding in the Conwy Estuary by collating all available documented events into one space together with the driving river flow and sea level conditions and their relative timings. We believe that similar circumstances of incomplete historical records of estuary flooding are widespread nationally and indeed there is limited knowledge of how estuary flooding has varied geographically. National UK chronologies of flash flooding (Archer et al., 2021) and coastal flooding (Haigh et al., 2015) have been compiled, but such records do not exist for estuaries.

Documenting compound flood events aids in understanding and analysing the drivers, interactions, and impacts of the hazards (Haigh et al., 2015; Haigh et al., 2017), validating numerical and statistical techniques, and calculating optimal thresholds. Recording historic information on river flows/levels, sea levels, other sources such as pluvial and groundwater flows, and subsequent flooded areas helps to identify high-risk areas and areas where appropriate measures to reduce future flood risk may be required. This prior knowledge combined with current information on where and when certain combinations of extreme conditions are forecast can aid in incident response for flood agencies and emergency services, and help local authorities identify what resources are needed in the short and longer term following flooding. Comprehensive historic flooding records can provide an opportunity to assess the effectiveness of existing flood management policies and flood control measures, such as floodwalls or drainage systems, that need improvement. This knowledge can guide future engineering designs for a range of coastal development, ensuring the construction of more resilient and adaptive infrastructure that can better withstand flood events. Documenting flood events can also build a database of information to help to raise public awareness of and resilience to flood hazards. Photographs, videos, and written accounts of past events can evoke an emotional response to prompt individuals and communities to engage with future flood preparedness and evacuation plans (Fekete et al., 2021; Wolff, 2021). This data could also be extended to include storm tracks, storm footprints, rainfall intensity, groundwater levels, and catchment saturation to build a greater understanding of the meteorological conditions that can contribute to compound flooding events (Zong et al., 2003). Social media data, including geolocated tweets, have been used to identify the remarkability of events and highlight major cities, including Miami, New York, and Boston, that are vulnerable to flooding (Moore and Obradovich, 2020). Qualitative hazard data from archived and digitised newspaper articles has been extracted to identify geographic location, date, triggers and damages of estuarine floods (Rilo et al., 2022) and validate flood models (Yagoub et al., 2020).

The combined approach to identify driver-thresholds for compound flooding presented here, and additional parameters suggested to develop the approach, relies on availability and access to sufficient instrumental data at the appropriate temporal resolution, and topographical and bathymetric data at appropriate spatial resolution. The UK sea levels, river discharges, and topography are recorded, archived, and accessed via national government and research agencies (e.g. British Oceanographic Data Centre, National River Flow Archive, Centre for Environment, Fisheries and Aquaculture Science, and Channel Coastal Observatory). However, nearly 50% of the world's coastal waters remain unsurveyed (IHO C-55, 2021), and 290 tide gauges that form the Global Sea Level Observing System (GLOSS, Merrifield et al., 2009) are unevenly distributed across the globe and do not account for local, vertical land movements. The approach described here could supplement existing observation systems with new technologies to improve records of coastal processes (Marcos et al., 2019), at local scales including X-band radar derived intertidal bathymetries (Bell et al., 2015; Bird et al., 2020), X-band radar derived tide and surge (Costa et al., 2022), and regional scales including Satellite-Derived Bathymetry (Cesbron et al., 2021 and Hasan and Matin, 2022), and satellite altimetry (Cipollini et al., 2019), which measures the sea level from space with sufficiently dense global coverage. Global model projections of storm surge and tide can be downscaled and applied to inform assessment of coastal flood impacts (Muis et al., 2023). Temporal and spatial gaps also occur in the global river discharge observing network, and hydrometric data are not available in real time (Lavers et al., 2019; Harrigan et al., 2020). Research has focused on coupling surface and sub-surface runoff models, hydrologic models, and land surface models, forced with global atmospheric reanalysis (e.g. ECMWF's ERA5) to produce river discharge reanalysis (Harrigan et al., 2020). Combining observation and downscaled modelled data to explore thresholds for estuarine flooding is one approach to apply this methodology worldwide.

Improving the resilience and preparedness of communities to flood hazard is a UK priority policy, as outlined in the Defra Policy Statement on Flooding (2020), and highlights the need for integrated approaches to flood hazard management. Instrumental data can be used in conjunction with earth observation records, including remote sensing and satellite imagery, of flooding to build more comprehensive databases of past records of estuarine flooding and be supported with numerical modelling studies to help identify thresholds for flooding (Heimhuber et al. 2021; Costa et al. 2023).

4.3 Future changes in flooding

Extreme sea levels for the Conwy, comprising large spring tides and large skew surges, could reach ~6 m (OD) and were simulated here in the upper rows of the scenario parameter space. These levels have not yet been seen in the Conwy but could happen presently. The *FloodArea* contours are close together in this section of the parameter space and show that relatively small increases in sea level and/or river flows lead to large increases in flood extent. This section of the parameter space is likely to become more relevant in the coming decades, as a result of sea-level rise and projected increases in the magnitudes of peak river flow events under future climate conditions. Sea-level rise and geomorphic changes will lead to a new baseline for flooding and new driver-thresholds and interactions. Many studies have started to consider the impact of climate change on compound estuary flooding (Robins et al., 2016; Ghanbari et al. 2021). Outputs of climate models were analysed to show that changes in sea level and precipitation can substantially increase the likelihood of a compound event, where a 100-year event could become a 3-year event by 2100 (Sheng et al., 2022). Model simulations of synthetic storms of combined tropical cyclones and sea-level rise in Cape Fear Estuary, North Carolina, have shown that future climatology will increase a 100-year flood extent by 27 % (Gori and Lin, 2022). In addition to future changes in drivers of compound events, it is possible that changes in storm tracks will influence the clustering and timing of events (Haigh et al. 2016; Eichentopf et al. 2019), and changes in land use could influence groundwater saturation, baseflow, and overall floodwater storage and drainage capacity of the system (Rahimi et al., 2020). However, uncertainties in future UK projections of river discharge and sea-level must be accounted for when considering compound flood effects (Lane et al., 2022). It is beyond the scope of this research to explore the influence of future climate changes on thresholds but could be explored by running simulations with different groundwater saturation, clustered events, and higher sea level or river discharge behaviours. A better understanding of how compound events and thresholds will change in the future is also crucial for developing adaptive strategies for high-impact events (Zscheischler et al., 2018), and climate projections of changing sea level, storm surge, river discharge, and storm tracks should be considered in model scenarios.

5 Conclusion

The urbanisation and industrialisation of estuaries have increased the vulnerability of communities to extreme events, such as flooding from high sea levels and river discharge. The impacts of these events are further amplified when extreme sea/river events occur simultaneously. Flooding occurs when coastal or fluvial conditions exceed critical thresholds such as flood defence heights, so there is a need to identify the driving land and sea conditions under which these thresholds are exceeded and the type of flooding that ensues. This research developed a novel framework that utilised a combination of historic estuary flooding records, instrumental monitoring data, numerical modelling, and probabilistic analyses to identify driver-thresholds for compound flooding, for an estuary that is especially vulnerable to compound flooding events (Conwy, N-Wales, UK).

The simulations predict how the total estuary flooding extent responds to the magnitude of river discharge, tide, and surge magnitude, and the timing of peak river discharge relative to tidal high water. Most flooding occurs when one or both sea level and river discharge drivers are extreme (e.g., >85th percentiles), but with amplified (compounding) flooding under relatively moderate circumstances (e.g. 60-70th and 30-50th percentiles) and in specific regions of the estuary (mid-estuary). Flooding is sensitive to a change in the timing of peak river discharge relative to tidal high water, with a –3 hour time lag (peak river discharge three hours before high water and coinciding with a rising tide that ‘traps in’ the freshwater) causing 7.7 % more flooding across the parameter space than with a 0 hour lag. There is spatial variability in flooding that is dependent on the combination and magnitude of the drivers. We show in detail the simulated extent of flooding in the lower estuary under extreme sea level conditions, and in the upper-estuary from extreme river flow conditions – and the spatially intricate nature of flooding throughout the estuary under combined moderate and extreme (‘worst-case’) sea level and river flows.

The research highlights that the recorded flooding extents held by national agencies are incomplete. This database is important to build knowledge on past flooding episodes (e.g., when and where has flooded, and under what conditions), undertake further analyses such as temporal trends in flooding, and develop accurate and timely flood warnings. The historic flooding record for the Conwy was supplemented with information obtained from online sources available 2004-2022, and set within the context of the most extreme 100 compound events during the period 1980-2022. An estuary inundation model was then used to ‘fill’ the parameter space of possible compound events (1560 separate simulations). This combined approach of modelling referenced to historic flooding events allowed us to identify a range of thresholds for flooding.

The results highlight under which conditions flooding is predicted to occur, or not, throughout the estuary, and identify driver-thresholds for flooding that are relevant to historic recorded flooding, steep increases in flooding (sensitive tipping-points), and location-specific/impact-specific flooding. The method can be used to enhance our understanding of estuarine flooding dynamics and improve flood risk assessments – it can be applied to other estuaries worldwide where there are paired coastal and fluvial monitoring/model data, and the methodology can be developed to include additional drivers and changes in the timing of behaviour of the drivers surges under different climate/management conditions.

Code availability

All code can be provided by the corresponding authors upon request.

Data availability

All raw data can be provided by the corresponding authors upon request.

Author contribution

CL, NC, GV, PR, AB, and TC formulated the research and developed the methodology; GV and TC developed, calibrated, and validated the model setup; NC ran the model and managed model outputs; AO, SM, MR contributed to data analysis; CL, NC, and PR analysed and visualised results; CL wrote the manuscript draft; PR, NC, GV, AB, TC, AO contributed to, reviewed, and edited the manuscript.

Competing Interests

The authors declare that they have no conflict of interest.

Acknowledgements

The authors wish to acknowledge the NERC-UK Climate Resilience Programme project 'SEARCH (NE/V004239/1)', in partnership with Jason Lowe, Rachel Perks, Jonathan Tinker, and Jennifer Pirret at the Met Office; Mark Pugh at Natural Resources Wales; Sue Manson and Harriet Orr at the Environment Agency; and Fiona McLay at the Scottish Environment Protection Agency. The authors also acknowledge Cllr Aaron Wynne at Conwy County Borough Council and John Owen and Robert Meyer who are residents and landowners in the Conwy floodplains, for their knowledge on flooding in the region.

References

Abbasian, M.S.; Jalali, S.; Mousavi Nadoushani, S.S.: Multivariate Flood Frequency Analysis Using Copula with Parametric and Nonparametric Marginal Distribution Function. MCEJ., 14 (4), 81-92, http://mcej.modares.ac.ir/article-16-10840-en.html, 2015.

Alfieri, L., Feyen, L., Salamon, P., Thielen, J., Bianchi, A., Dottori, F., and Burek, P.: Modelling the socio-economic impact of river floods in Europe, Nat. Hazards Earth Syst. Sci., 16, 1401–1411, https://doi.org/10.5194/nhess-16-1401-2016, 2016.

Alfieri, L., Salamon, P., Pappenberger, F., Wetterhall, F., and Thielen, J.: Operational early warning systems for water-related hazards in Europe, Environmental Science & Policy, 21, 35–49, https://doi.org/10.1016/j.envsci.2012.01.008, 2012.

Akoglu, H.: User's guide to correlation coefficients, Turkish Journal of Emergency Medicine, 18, 91–93, https://doi.org/10.1016/j.tjem.2018.08.001, 2018.

Archer, D., O'Donnell, G., Lamb, R., Warren, S., and Fowler, H. J.: Historical flash floods in England: New regional chronologies and database, J Flood Risk Management, 12, https://doi.org/10.1111/jfr3.12526, 2019.

Arns, A., Wahl, T., Wolff, C., Vafeidis, A. T., Haigh, I. D., Woodworth, P., Niehüser, S., & Jensen, J.: Non-linear interaction modulates global extreme sea levels, coastal flood exposure, and impacts. Nature Communications, 11(1). https://doi.org/10.1038/s41467-020-15752-5, 2020.

Bates, P. D., Horritt, M. S., & Fewtrell, T. J.: A simple inertial formulation of the shallow water equations for efficient two-dimensional flood Inundation modelling. Journal of Hydrology, 387(1-2), 33-45. https://doi.org/10.1016/j.jhydrol.2010.03.027, 2010.

BBC: National Eisteddfod: Flooding worries over Llanrwst site: https://www.bbc.co.uk/news/uk-wales-47666319, last access: April 2023, 2019.

BBC: Storm Ciara: Dramatic scenes across Wales: https://www.bbc.co.uk/news/uk-wales-51434782, last access: April 2023, 2020.

Bilskie, M. V. and Hagen, S. C.: Defining Flood Zone Transitions in Low-Gradient Coastal Regions, Geophysical Research Letters, 45, 2761–2770, https://doi.org/10.1002/2018gl077524, 2018.

Bird, C.O., Bell, P.S., Plater, A.J.: Application of marine radar to monitoring seasonal and event-based changes in intertidal morphology. Geomorphology. 285, 1–15, https://doi.org/10.1016/j.geomorph.2017.02.002, 2017.

Camus, P., Haigh, I. D., Nasr, A. A., Wahl, T., Darby, S. E., and Nicholls, R. J.: Regional analysis of multivariate compound coastal flooding potential around Europe and environs: sensitivity analysis and spatial patterns, Nat. Hazards Earth Syst. Sci., 21, 2021–2040, https://doi.org/10.5194/nhess-21-2021-2021, 2021.

Cai, H., Savenije, H. H. G., and Toffolon, M.: Linking the river to the estuary: influence of river discharge on tidal damping, Hydrol. Earth Syst. Sci., 18, 287–304, https://doi.org/10.5194/hess-18-287-2014, 2014.

Census: Coastal towns in England and Wales: October 2020: https://www.ons.gov.uk/businessindustryandtrade/tourismindustry/articles/coastaltownsinenglandandwales/2020-10-06, last access: May 2023, 2020.

Cesbron, G., Melet, A., Almar, R., Lifermann, A., Tullot, D., Crosnier, L.: Pan-European Satellite-Derived Coastal Bathymetry—Review, User Needs and Future Services. Frontiers in Marine Science. 8, https://doi.org/10.3389/fmars.2021.740830, 2021.

Chilton, D., Hamilton, D. P., Nagelkerken, I., Cook, P., Hipsey, M. R., Reid, R., Sheaves, M., Waltham, N. J., and Brookes, J.: Environmental Flow Requirements of Estuaries: Providing Resilience to Current and Future Climate and Direct Anthropogenic Changes, Front. Environ. Sci., 9, https://doi.org/10.3389/fenvs.2021.764218, 2021.

Chow, V.T., Maidment, D.R. and Mays, L.W. (1988) Applied Hydrology. International Edition, McGraw-Hill Book Company, New York.

Cipollini, P., Calafat, F.M., Jevrejeva, S., Melet, A., Prandi, P.: Monitoring Sea Level in the Coastal Zone with Satellite Altimetry and Tide Gauges. Surveys in Geophysics. 38(1), 33–57, https://doi.org/10.1007/s10712-016-9392-0, 2016.

Coles, S.: An Introduction to Statistical Modeling of Extreme Values. Springer, London. https://doi.org/10.1007/978-1-4471-3675-0, 2001.

Costa, W. L. L., Bryan, K. R., and Coco, G.: Modelling extreme water levels using intertidal topography and bathymetry derived from multispectral satellite images, Nat. Hazards Earth Syst. Sci., 23, 3125–3146, https://doi.org/10.5194/nhess-23-3125-2023, 2023.

Couasnon, A., Eilander, D., Muis, S., Veldkamp, T. I. E., Haigh, I. D., Wahl, T., Winsemius, H. C., and Ward, P. J.: Measuring compound flood potential from river discharge and storm surge extremes at the global scale, Nat. Hazards Earth Syst. Sci., 20, 489–504, https://doi.org/10.5194/nhess-20-489-2020, 2020.

Coulthard, T. J., Neal, J. C., Bates, P. D., Ramirez, J., de Almeida, G. A. M., and Hancock, G. R.: Integrating the LISFLOOD-FP 2D hydrodynamic model with the CAESAR model: implications for modelling landscape evolution, Earth Surf Processes Landf, 38, 1897–1906, https://doi.org/10.1002/esp.3478, 2013.

Cutter, S. L., Emrich, C. T., Morath, D. P., and Dunning, C. M.: Integrating social vulnerability into federal flood risk management planning, J Flood Risk Management, 6, 332–344, https://doi.org/10.1111/jfr3.12018, 2013.

Defra: Flood and coastal erosion risk management Policy Statement:https://www.gov.uk/government/publications/flood-and-coastal-erosion-risk-management-policy-statement, last access: November 2021.

Environment Agency: Reliability in Flood Incident Management Planning Final Report – Part A: Guidance Science project SC060063/SR1: https://assets.publishing.service.gov.uk/media/602e8e04d3bf7f722294d1d1/Reliability_in_Flood_Incident_Management_guidance.pdf, last access: November 2021, 2009.

Environment Agency: National flood and coastal erosion risk management strategy for England: executive summary: https://www.gov.uk/government/publications/national-flood-and-coastal-erosion-risk-management-strategy-for-england--2/national-flood-and-coastal-erosion-risk-management-strategy-for-england-executive-summary, last access: November 2021, 2020.

Environment Agency: State of the environment: the coastal and marine environment: https://assets.publishing.service.gov.uk/government/uploads/system/uploads/attachment_data/file/1130743/State_of_the_environment_-_the_coastal_and_marine_environment_-_report.pdf, last access: January 2023.

Eichentopf, S., Karunarathna, H., and Alsina, J. M.: Morphodynamics of sandy beaches under the influence of storm sequences: Current research status and future needs, Water Science and Engineering, 12, 221–234, https://doi.org/10.1016/j.wse.2019.09.007, 2019.

Eilander, D., Couasnon, A., Leijnse, T., Ikeuchi, H., Yamazaki, D., Muis, S., Dullaart, J., Haag, A., Winsemius, H. C., and Ward, P. J.: A globally applicable framework for compound flood hazard modeling, Nat. Hazards Earth Syst. Sci., 23, 823–846, https://doi.org/10.5194/nhess-23-823-2023, 2023.

Elliott, L. R., White, M. P., Grellier, J., Rees, S. E., Waters, R. D., and Fleming, L. E.: Recreational visits to marine and coastal environments in England: Where, what, who, why, and when?, Marine Policy, 97, 305–314, https://doi.org/10.1016/j.marpol.2018.03.013, 2018.

Evans, O.: Storm Ciara: Llanrwst, Colwyn Bay and Llanfair TH hit by flooding as torrential rain causes chaos across Conwy: https://www.dailypost.co.uk/news/north-wales-news/storm-ciara-flooding-hits-communities-17715701, last access: April 2023

Familkhalili, R., Talke, S. A., and Jay, D. A.: Compound flooding in convergent estuaries: insights from an analytical model, Ocean Sci., 18, 1203–1220, https://doi.org/10.5194/os-18-1203-2022, 2022.

Fekete, A., Aslam, A. B., de Brito, M. M., Dominguez, I., Fernando, N., Illing, C. J., KC, A. K., Mahdavian, F., Norf, C., Platt, S., Santi, P. A., and Tempels, B.: Increasing flood risk awareness and warning readiness by participation – But who understands what under 'participation'?, International Journal of Disaster Risk Reduction, 57, 102157, https://doi.org/10.1016/j.ijdrr.2021.102157, 2021.

Feng, D., Tan, Z., Engwirda, D., Liao, C., Xu, D., Bisht, G., Zhou, T., Li, H.-Y., and Leung, L. R.: Investigating coastal backwater effects and flooding in the coastal zone using a global river transport model on an unstructured mesh, Hydrol. Earth Syst. Sci., 26, 5473–5491, https://doi.org/10.5194/hess-26-5473-2022, 2022.

Feng, D., Tan, Z., Xu, D., and Leung, L. R.: Understanding the compound flood risk along the coast of the contiguous United States, Hydrol. Earth Syst. Sci., 27, 3911–3934, https://doi.org/10.5194/hess-27-3911-2023, 2023.Ferranti, E., Chapman, L., and Whyatt, D.: A Perfect Storm? The collapse of Lancaster's critical infrastructure networks following intense rainfall on 4/5 December 2015, Weather, 72, 3–7, https://doi.org/10.1002/wea.2907, 2017.

FloodList: UK – Flood Rescues After Rivers Overflow in England and Wales: https://floodlist.com/europe/united-kingdom/rivers-overflow-england-wales-march-2019, last access: April 2023.

Ganguli, P. and Merz, B.: Extreme Coastal Water Levels Exacerbate Fluvial Flood Hazards in Northwestern Europe, Sci Rep, 9, https://doi.org/10.1038/s41598-019-49822-6, 2019.

Genest, C. and Favre, A.-C.: Everything You Always Wanted to Know about Copula Modeling but Were Afraid to Ask, J. Hydrol. Eng., 12, 347–368, https://doi.org/10.1061/(asce)1084-0699(2007)12:4(347), 2007.

Ghanbari, M., Arabi, M., Kao, S., Obeysekera, J., and Sweet, W.: Climate Change and Changes in Compound Coastal-Riverine Flooding Hazard Along the U.S. Coasts, Earth's Future, 9, https://doi.org/10.1029/2021ef002055, 2021.

Gori, A. and Lin, N.: Projecting Compound Flood Hazard Under Climate Change With Physical Models and Joint Probability Methods, Earth's Future, 10, https://doi.org/10.1029/2022ef003097, 2022.

Greenwood, C, and Nikulin, M.S.: A guide to chi-squared testing, Wiley. New York ISBN 0-471-55779-X, 1996.

Gupta, H. V., Kling, H., Yilmaz, K. K., and Martinez, G. F.: Decomposition of the mean squared error and NSE performance criteria: Implications for improving hydrological modelling, Journal of Hydrology, 377, 80–91, https://doi.org/10.1016/j.jhydrol.2009.08.003, 2009.

The First Global Integrated Marine Assessment, Cambridge University Press, https://doi.org/10.1017/9781108186148, 2017.

Haigh, I. D., Wadey, M. P., Gallop, S. L., Loehr, H., Nicholls, R. J., Horsburgh, K., Brown, J. M., and Bradshaw, E.: A user-friendly database of coastal flooding in the United Kingdom from 1915–2014, Sci Data, 2, https://doi.org/10.1038/sdata.2015.21, 2015.

Haigh, I. D., Wadey, M. P., Wahl, T., Ozsoy, O., Nicholls, R. J., Brown, J. M., Horsburgh, K., and Gouldby, B.: Spatial and temporal analysis of extreme sea level and storm surge events around the coastline of the UK, Sci Data, 3, https://doi.org/10.1038/sdata.2016.107, 2016.

Haigh, I. D., Ozsoy, O., Wadey, M. P., Nicholls, R. J., Gallop, S. L., Wahl, T., and Brown, J. M.: An improved database of coastal flooding in the United Kingdom from 1915 to 2016, Sci Data, 4, https://doi.org/10.1038/sdata.2017.100, 2017.

Harrigan, S., Zsoter, E., Alfieri, L., Prudhomme, C., Salamon, P., Wetterhall, F., Barnard, C., Cloke, H., Pappenberger, F.: GloFAS-ERA5 operational global river discharge reanalysis 1979–present. Earth System Science Data. 12(3), 2043–2060, https://doi.org/10.5194/essd-12-2043-2020, 2020.

Harrison, L. M., Coulthard, T. J., Robins, P. E., and Lewis, M. J.: Sensitivity of Estuaries to Compound Flooding, Estuaries and Coasts, 45, 1250–1269, https://doi.org/10.1007/s12237-021-00996-1, 2021.

Hasan, G.M.J., Matin, N.: Intertidal bathymetry and foreshore slopes derived from satellite images for static coasts. Regional Studies in Marine Science. 51, 102233, https://doi.org/10.1016/j.rsma.2022.102233, 2022.

Heimhuber, V., Vos, K., Fu, W., Glamore, W.: InletTracker: An open- source Python toolkit for historic and near real-time monitoring of coastal inlets from Landsat and Sentinel-2, Geomorphology, 389, https://doi.org/10.1016/j.geomorph.2021.107830, 2021.

Hendry, A., Haigh, I. D., Nicholls, R. J., Winter, H., Neal, R., Wahl, T., Joly-Laugel, A., and Darby, S. E.: Assessing the characteristics and drivers of compound flooding events around the UK coast, Hydrol. Earth Syst. Sci., 23, 3117–3139, https://doi.org/10.5194/hess-23-3117-2019, 2019.

Hoitink, A. J. F. and Jay, D. A.: Tidal river dynamics: Implications for deltas, Reviews of Geophysics, 54, 240–272, https://doi.org/10.1002/2015rg000507, 2016.

Holgate, S.J., Matthews, A., Woodworth, P.L., Rickards, L.J., Tamisiea, M.E., Bradshaw, E., Foden, P.R., Gordon, K.M., Jevrejeva, S., Pugh, J.: New Data Systems and Products at the Permanent Service for Mean Sea Level. Journal of Coastal Research. 29(3), 493, https://doi.org/10.2112/JCOASTRES-D-12-00175.1, 2013.

Howlett, E. R., Bowers, D. G., Malarkey, J., and Jago, C. F.: Stratification in the presence of an axial convergent front: Causes and implications, Estuarine, Coastal and Shelf Science, 161, 1–10, https://doi.org/10.1016/j.ecss.2015.04.003, 2015.

HR Wallingford: Conwy Tidal Flood Risk Assessment: http://conwyfloodmap.hrwallingford.co.uk/report/HRWallingford_ConwyFRA_Stage1_Report_EX4667.pdf, last access: April 2023, 2008.

IHO C-55: Publication C-55 “Status of Hydrographic Surveying and Charting Worldwide.”. Monte Carlo: IHO, https://iho.int/en/iho-c-55, 2021.

Ikeuchi, H., Hirabayashi, Y., Yamazaki, D., Kiguchi, M., Koirala, S., Nagano, T., Kotera, A., Kanae, S.: Modeling complex flow dynamics of fluvial floods exacerbated by sea level rise in the Ganges–Brahmaputra–Meghna Delta. Environ. Res. Lett. 10 124011, https://doi.org/10.1088/1748-9326/10/12/124011, 2015.

ITV: Flood warnings as downpours and high tides hit Wales: https://www.itv.com/news/wales/2015-12-26/flood-warnings-at-downpours-and-high-tides-hit-wales, last access: April 2023, 2015.

Jago, C., Robins, P., Howlett, E., Hassard, F., Rajko-Nenow, P., Jackson, S., Chien, N., & Malham, S.: Trapping and bypassing of suspended particulate matter, particulate nutrients and faecal indicator organisms in the River-Estuary transition zone of a shallow Macrotidal Estuary. Science of The Total Environment (in review).

Jones, M.: Boxing Day floods 2015: How North Wales ground to a halt during the deluge: https://www.dailypost.co.uk/news/north-wales-news/boxing-day-floods-2015-how-12370017, last access: May 2023, 2015.

Juárez, B., Stockton, S. A., Serafin, K. A., and Valle-Levinson, A.: Compound Flooding in a Subtropical Estuary Caused by Hurricane Irma 2017, Geophysical Research Letters, 49, https://doi.org/10.1029/2022gl099360, 2022.

Khajehei, S., Ahmadalipour, A., and Moradkhani, H.: An effective post-processing of the North American multi-model ensemble (NMME) precipitation forecasts over the continental US, Clim Dyn, 51, 457–472, https://doi.org/10.1007/s00382-017-3934-0, 2017.

Khanam, M., Sofia, G., Koukoula, M., Lazin, R., Nikolopoulos, E. I., Shen, X., and Anagnostou, E. N.: Impact of compound flood event on coastal critical infrastructures considering current and future climate, Nat. Hazards Earth Syst. Sci., 21, 587–605, https://doi.org/10.5194/nhess-21-587-2021, 2021.

Khojasteh, D., Glamore, W., Heimhuber, V., and Felder, S. Sea level rise impacts on estuarine dynamics: A review. Science of the Total Environment, 780, https://doi.org/10.1016/j.scitotenv.2021.146470, 2021.

Lavers, D., Harrigan, S., Andersson, E., Richardson, D. S., Prudhomme, C., and Pappenberger, F.: A vision for improving global flood forecasting, Environ. Res. Lett., 14, 121002, https://doi.org/10.1088/1748-9326/ab52b2, 2019.

Lane, R. A., Coxon, G., Freer, J., Seibert, J., and Wagener, T.: A large-sample investigation into uncertain climate change impacts on high flows across Great Britain, Hydrol. Earth Syst. Sci., 26, 5535–5554, https://doi.org/10.5194/hess-26-5535-2022, 2022.

Lindeboom, H. The Coastal Zone: An Ecosystem Under Pressure. In Oceans 2020: Science, Trends and the Challenge of Sustainability; Field, J.G., Hempel, G., Summerhayes, C.P., Eds.; Island Press: Washington, DC, USA; pp. 49–84. ISBN 1-55963-470-7, 2002

Lyddon, C., Brown, J. M., Leonardi, N., and Plater, A. J.: Flood Hazard Assessment for a Hyper-Tidal Estuary as a Function of Tide-Surge-Morphology Interaction, Estuaries and Coasts, 41, 1565–1586, https://doi.org/10.1007/s12237-018-0384-9, 2018.

Lyddon, C. E., Brown, J. M., Leonardi, N., Saulter, A., and Plater, A. J.: Quantification of the Uncertainty in Coastal Storm Hazard Predictions Due to Wave-Current Interaction and Wind Forcing, Geophysical Research Letters, 46, 14576–14585, https://doi.org/10.1029/2019gl086123, 2019.

Lyddon, C., Robins, P., Lewis, M., Barkwith, A., Vasilopoulos, G., Haigh, I., and Coulthard, T.: Historic Spatial Patterns of Storm-Driven Compound Events in UK Estuaries, Estuaries and Coasts, 46, 30–56, https://doi.org/10.1007/s12237-022-01115-4, 2022.

Marcos, M., Wöppelmann, G., Matthews, A., Ponte, R.M., Birol, F., Ardhuin, F., Coco, G., Santamaría-Gómez, A., Ballu, V., Testut, L., Chambers, D., Stopa, J.E.: Coastal Sea Level and Related Fields from Existing Observing Systems. Surveys in Geophysics. 40(6), 1293–1317, https://doi.org/10.1007/s10712-019-09513-3, 2019.

Matthews, T., Murphy, C., McCarthy, G., Broderick, C., and Wilby, R. L.: Super Storm Desmond: a process-based assessment, Environ. Res. Lett., 13, 014024, https://doi.org/10.1088/1748-9326/aa98c8, 2018.

Met Office: Stormy and very wet spell March 2019: https://www.metoffice.gov.uk/binaries/content/assets/metofficegovuk/pdf/weather/learn-about/uk-past-events/interesting/2019/2019_004_stormy_spell.pdf last access: May 2023, 2019.

Moftakhari, H. R., Salvadori, G., AghaKouchak, A., Sanders, B. F., and Matthew, R. A.: Compounding effects of sea level rise and fluvial flooding, Proc. Natl. Acad. Sci. U.S.A., 114, 9785–9790, https://doi.org/10.1073/pnas.1620325114, 2017.

Moore, F. C. and Obradovich, N.: Using remarkability to define coastal flooding thresholds, Nat Commun, 11, https://doi.org/10.1038/s41467-019-13935-3, 2020.

Moradian, S., Olbert, A. I., Gharbia, S., and Iglesias, G.: Copula-based projections of wind power: Ireland as a case study, Renewable and Sustainable Energy Reviews, 175, 113147, https://doi.org/10.1016/j.rser.2023.113147, 2023.

Muis, S., Verlaan, M., Winsemius, H. C., Aerts, J. C. J. H., and Ward, P. J.: A global reanalysis of storm surges and extreme sea levels, Nat Commun, 7, https://doi.org/10.1038/ncomms11969, 2016.

Muis, S., Apecechea, M. I., Dullaart, J., de Lima Rego, J., Madsen, K. S., Su, J., Yan, K., and Verlaan, M.: A High-Resolution Global Dataset of Extreme Sea Levels, Tides, and Storm Surges, Including Future Projections, Front. Mar. Sci., 7, https://doi.org/10.3389/fmars.2020.00263, 2020.

Muis, S., Aerts, J.C.J.H., Á. Antolínez, J.A., Dullaart, J.C., Duong, T.M., Erikson, L., Haarsma, R.J., Apecechea, M.I., Mengel, M., Le Bars, D., O'Neill, A., Ranasinghe, R., Roberts, M.J., Verlaan, M., Ward, P.J., Yan, K. (2023) Global Projections of Storm Surges Using High-Resolution CMIP6 Climate Models. Earth's Future. 11(9), https://doi.org/10.1029/2023EF003479, 2023.

Nasr, A. A., Wahl, T., Rashid, M. M., Camus, P., and Haigh, I. D.: Assessing the dependence structure between oceanographic, fluvial, and pluvial flooding drivers along the United States coastline, Hydrol. Earth Syst. Sci., 25, 6203–6222, https://doi.org/10.5194/hess-25-6203-2021, 2021.

Natural Resource Wales Flood Investigation Report: Llanrwst Flooding December 2015 [online] Available at: https://naturalresources.wales/media/678788/flood-investigation-report-llanrwst-2015-english.pdf last access: November 2022, 2016.

Natural Resource Wales: DataMap Wales: Recorded Flood Extents (Formerly Lle): https://datamap.gov.wales/layers/inspire-nrw:NRW_HISTORIC_FLOODMAP last access: November 2022, 2020.

Natural Resource Wales: Historic Flood Map: https://datamap.gov.wales/maps/new?layer=inspire-nrw:NRW_HISTORIC_FLOODMAP#/ last access: January 2023.

National Coastal Tourism Academy: Coastal Tourism: https://coastaltourismacademy.co.uk/coastal-tourism last access: August 2023.

Neal, J., Hawker, L., Savage, J., Durand, M., Bates, P., and Sampson, C.: Estimating River Channel Bathymetry in Large Scale Flood Inundation Models, Water Resources Research, 57, https://doi.org/10.1029/2020wr028301, 2021.

Nelsen, Roger B.: An introduction to Copulas. Springer Series in Statistics. Second edition. Department of Mathematical Sciences. Lewis & Clark College, MSC 110, ISBN 978-0-387-28678-5, 2007.

O'Donnell, E. C. and Thorne, C. R.: Drivers of future urban flood risk, Phil. Trans. R. Soc. A., 378, 20190216, https://doi.org/10.1098/rsta.2019.0216, 2020.

Olbert, A. I., Moradian, S., Nash, S., Comer, J., Kazmierczak, B., Falconer, R. A., and Hartnett, M.: Combined statistical and hydrodynamic modelling of compound flooding in coastal areas - Methodology and application, Journal of Hydrology, 620, 129383, https://doi.org/10.1016/j.jhydrol.2023.129383, 2023.

ONR: ONR Expert Panel on Natural Hazards, Analysis of Coastal Flood Hazards for Nuclear Sites: 2021 https://www.onr.org.uk/operational/tech_asst_guides/ns-tast-gd-013-annex-3-reference-paper.docx, Last access: October 2023, 2021.

Pawlowicz, R., Beardsley, B., and Lentz, S.: Classical tidal harmonic analysis including error estimates in MATLAB using T_TIDE, Computers & Geosciences, 28, 929–937, https://doi.org/10.1016/s0098-3004(02)00013-4, 2002.

Peter Sheng, Y., Paramygin, V. A., Yang, K., and Rivera-Nieves, A. A.: A sensitivity study of rising compound coastal inundation over large flood plains in a changing climate, Sci Rep, 12, https://doi.org/10.1038/s41598-022-07010-z, 2022.

Penning-Rowsell, E. C.: A realistic assessment of fluvial and coastal flood risk in England and Wales, Trans Inst British Geog, 40, 44–61, https://doi.org/10.1111/tran.12053, 2014.

Pugh, D.T. Tides, surges and mean sea-level (reprinted with corrections), Chichester, UK. John Wiley & Sons, Ltd, 1996.

Rahimi, R., Tavakol-Davani, H., Graves, C., Gomez, A., and Fazel Valipour, M.: Compound Inundation Impacts of Coastal Climate Change: Sea-Level Rise, Groundwater Rise, and Coastal Precipitation, Water, 12, 2776, https://doi.org/10.3390/w12102776, 2020.

Rilo, A., Tavares, A. O., Freire, P., Zêzere, J. L., and Haigh, I. D.: Improving Estuarine Flood Risk Knowledge through Documentary Data Using Multiple Correspondence Analysis, Water, 14, 3161, https://doi.org/10.3390/w14193161, 2022.

Robins, P. E., Neill, S. P., and Giménez, L.: A numerical study of marine larval dispersal in the presence of an axial convergent front, Estuarine, Coastal and Shelf Science, 100, 172–185, https://doi.org/10.1016/j.ecss.2012.02.001, 2012.

Robins, P. E., Skov, M. W., Lewis, M. J., Giménez, L., Davies, A. G., Malham, S. K., Neill, S. P., McDonald, J. E., Whitton, T. A., Jackson, S. E., and Jago, C. F.: Impact of climate change on UK estuaries: A review of past trends and potential projections, Estuarine, Coastal and Shelf Science, 169, 119–135, https://doi.org/10.1016/j.ecss.2015.12.016, 2016.

Robins, P. E., Lewis, M. J., Elnahrawi, M., Lyddon, C., Dickson, N., and Coulthard, T. J.: Compound Flooding: Dependence at Sub-daily Scales Between Extreme Storm Surge and Fluvial Flow, Front. Built Environ., 7, https://doi.org/10.3389/fbuil.2021.727294, 2021.

Sadegh, M., Ragno, E., and AghaKouchak, A.: Multivariate Copula Analysis Toolbox (MvCAT): Describing dependence and underlying uncertainty using a Bayesian framework, Water Resources Research, 53, 5166–5183, https://doi.org/10.1002/2016wr020242, 2017.

Sadegh, M., Moftakhari, H., Gupta, H. V., Ragno, E., Mazdiyasni, O., Sanders, B., Matthew, R., and AghaKouchak, A.: Multihazard Scenarios for Analysis of Compound Extreme Events, Geophysical Research Letters, 45, 5470–5480, https://doi.org/10.1029/2018gl077317, 2018.

Šakić Trogrlić, R., van den Homberg, M., Budimir, M., McQuistan, C., Sneddon, A., and Golding, B.: Early Warning Systems and Their Role in Disaster Risk Reduction, Towards the "Perfect" Weather Warning, 11–46, https://doi.org/10.1007/978-3-030-98989-7_2, 2022.

Sene, K.: Thresholds. In: Flood Warning, Forecasting and Emergency Response. Springer, Berlin, Heidelberg. https://doi.org/10.1007/978-3-540-77853-0_3, 2008.

Skinner, C. J., Coulthard, T. J., Parsons, D. R., Ramirez, J. A., Mullen, L., and Manson, S.: Simulating tidal and storm surge hydraulics with a simple 2D inertia based model, in the Humber Estuary, U.K, Estuarine, Coastal and Shelf Science, 155, 126–136, https://doi.org/10.1016/j.ecss.2015.01.019, 2015.

Sklar.: Fonctions de répartition à n dimensions et leurs marges. Publications de l'Institut de Statistique de l'Université de Paris, 8. 229–231, 1959.

Sibley, A., Cox, D., and Titley, H.: Coastal flooding in England and Wales from Atlantic and North Sea storms during the 2013/2014 winter, Weather, 70, 62–70, https://doi.org/10.1002/wea.2471, 2015.

Spridgeon, D.: Aberconwy AM to ask emergency questions over Conwy Valley flooding: https://www.northwalespioneer.co.uk/news/18222471.aberconwy-ask-emergency-questions-conwy-valley-flooding/ last access: April 2023, 2020.

Svensson, C. and Jones, D. A.: Dependence between sea surge, river flow and precipitation in south and west Britain, Hydrol. Earth Syst. Sci., 8, 973–992, https://doi.org/10.5194/hess-8-973-2004, 2004.

Vasilopoulos, G., Coulthard, T., Robins, P., Lyddon, C., Barkwith, A., Chien, N., and Lewis, M.: Development and validation of flood inundation models for estuaries, EGU General Assembly 2023, Vienna, Austria, 23–28 Apr 2023, EGU23-5858, https://doi.org/10.5194/egusphere-egu23-5858, 2023.

Wang, X., Verlaan, M., Apecechea, M. I., and Lin, H. X.: Parameter estimation for a global tide and surge model with a memory-efficient order reduction approach, Ocean Modelling, 173, 102011, https://doi.org/10.1016/j.ocemod.2022.102011, 2022.

Ward, P. J., Couasnon, A., Eilander, D., Haigh, I. D., Hendry, A., Muis, S., Veldkamp, T. I. E., Winsemius, H. C., and Wahl, T.: Dependence between high sea-level and high river discharge increases flood hazard in global deltas and estuaries, Environ. Res. Lett., 13, 084012, https://doi.org/10.1088/1748-9326/aad400, 2018.

Welsh Government (2015) CABINET STATEMENT Coastal flooding – January 2014: https://www.gov.wales/written-statement-coastal-flooding-january-2014 last access: April 2023, 2014.

Welsh Government (2015) CABINET STATEMENT Flooding in North Wales December 2015: https://www.gov.wales/written-statement-flooding-north-wales-december-2015 last access: April 2023, 2015.

Wolff, E.: The promise of a "people-centred" approach to floods: Types of participation in the global literature of citizen science and community-based flood risk reduction in the context of the Sendai Framework, Progress in Disaster Science, 10, 100171, https://doi.org/10.1016/j.pdisas.2021.100171, 2021.

Wu, W., Westra, S., Leonard, M.: Estimating the probability of compound floods in estuarine regions. Hydrology and Earth System Sciences. 25(5), 2821–2841, 2021.

Xiao, Z., Yang, Z., Wang, T., Sun, N., Wigmosta, M., and Judi, D.: Characterizing the Non-linear Interactions Between Tide, Storm Surge, and River Flow in the Delaware Bay Estuary, United States, Front. Mar. Sci., 8, https://doi.org/10.3389/fmars.2021.715557, 2021.

Yagoub, M. M., Alsereidi, A. A., Mohamed, E. A., Periyasamy, P., Alameri, R., Aldarmaki, S., and Alhashmi, Y.: Newspapers as a validation proxy for GIS modeling in Fujairah, United Arab Emirates: identifying flood-prone areas, Nat Hazards, 104, 111–141, https://doi.org/10.1007/s11069-020-04161-y, 2020.

Yazdandoost, F., Moradian, S., Zakipour, M., Izadi, A., and Bavandpour, M.: Improving the precipitation forecasts of the North-American multi model ensemble (NMME) over Sistan basin, Journal of Hydrology, 590, 125263, https://doi.org/10.1016/j.jhydrol.2020.125263, 2020.

Zscheischler, J., Westra, S., van den Hurk, B. J. J. M., Seneviratne, S. I., Ward, P. J., Pitman, A., AghaKouchak, A., Bresch, D. N., Leonard, M., Wahl, T., and Zhang, X.: Future climate risk from compound events, Nature Clim Change, 8, 469–477, https://doi.org/10.1038/s41558-018-0156-3, 2018.

Zong, Y., Tooley, M.J. A.: Historical Record of Coastal Floods in Britain: Frequencies and Associated Storm Tracks. Natural Hazards 29, 13–36, https://doi.org/10.1023/A:1022942801531